Università degli Studi di Ferrara

ISTITUTO ITALIANO DI TECNOLOGIA

DOCTORAL COURSE IN
TRANSLATIONAL NEUROSCIENCE AND
NEUROTECHNOLOGIES

CYCLE XXXV

COORDINATOR Prof. FADIGA Luciano

MOVEMENT INTERMITTENCY IN SOCIAL COORDINATION

Scientific/Disciplinary Sector (SDS) BIO/09

Candidate

Dott. NAZZARO Giovanni

_____

Supervisor

Prof. D'AUSILIO Alessandro

_____

Prof. GRASSI Luigi

_____

Year 2019/2023

Table of contents

Acknowledgement

Al dottor Emanuele, all'amico Marco per avermi guidato e sostenuto come un fratello maggiore nonostante l'età in mio sfavore, a te devo la passione e l'abnegazione.

Al Prof. D'Ausilio e alla Dott.ssa Tomassini per la paziente, discreta e imprescindibile presenza, a voi devo l'arte che spero di aver imparato e messo da parte.

Al Prof. Fadiga per avermi concesso il piacere di una domanda e regalato il sostegno nel trovare una risposta, a lei devo la perseveranza e l'ambizione.

A tutti gli amici e colleghi del CTNSC per essere un porto sicuro di supporto e risate, a voi devo il legame e l'appartenenza.

A Ferrara per aver curato alcune mie inquietudini con la sua apparente domenica, a te devo i silenzi e la calma.

Agli amici di sempre per esserci immancabilmente nella gioia della condivisione, a voi devo l'affetto e l'ispirazione.

Alla mia famiglia per il supporto e conforto incondizionati in ogni mia scelta, a voi devo la fiducia e l'amore.

A Viola per cui ogni parola è superflua, a te devo la vita che ci siamo donati.

Abstract

Coordination of movements in humans has been extensively studied at a macroscopic level, such as the pacing of movements, particularly in tasks of interpersonal and bimanual coordination. However, by examining the fine structure of movement, another form of rhythmicity becomes apparent at a microscopic level. Movement is never completely smooth, but rather is organized into smaller units known as submovements, which appear as recurrent speed breaks occurring at faster timescales (2-3 Hz). These submovements may reflect intermittent feedback-based motor adjustments. To better understand the relationship between submovements in different coordination contexts, we characterized the timing of submovements emission in a series of rhythmic motor coordination task by asking participants to coordinate their index fingers either in-phase or anti-phase with themselves or with a real/virtual partner.

In Study 1, we analysed the temporal relationship between submovements emitted by both hands of a single participant during a bimanual coordination task. We also manipulated the availability of visual feedback to understand its impact on the emission of submovements, which are believed to reflect a vision based movement correction mechanism.

In Study 2, we explored the dynamics of submovements during interpersonal coordination, and thus with the goal of moving beyond their temporal emission in single individuals. In Study 3, we combined interpersonal and bimanual coordination into a single task by asking participants to coordinate with each other using both their hands.

In Study 4, we tested the validity of our results on mutual adaptation of submovements during interpersonal coordination by replacing one member of the pair with an unresponsive virtual partner. Finally, in Study 5, building on the ease of transferability of the previous task to clinical settings, we investigated the pattern of submovements emission in individuals with Parkinson's disease and cerebellar disorders to identify potentially new diagnostic markers and gain novel insights into the neural substrates underlying movement intermittency.

Overall, our results suggest that the mechanism responsible for the organization of movement into submovements is at least partly shared across different effectors, such as the two hands, and might be modulated by the availability and usability of visual and proprioceptive feedback. Moreover, the identification of different temporal patterns of

submovements emission leads us to conclude that the mechanisms controlling submovements production are highly flexible and tunable depending on the coordinative context. Submovements control can thus provide valuable insights into the low-level motor control mechanisms involved in achieving intra- and interpersonal motor coordination.

Finally, submovement-level control may serve as a novel objective marker of individual and social motor coordination capabilities that may be selectively impaired in some neurological and psychiatric conditions.

Chapter 1

Voluntary movement represents the fundamental interface with the world, the way we translate our intentions into actions to achieve goals and satisfy needs. The wide range of movements we are capable of results from the fine and coordinated regulation of the activity of approximately 640 skeletal muscles controlled by motor systems. The complex hierarchical and parallel architecture of the motor system contributes to the extreme variability and sophistication of our behavioural repertoire. Successful behaviours demand continuous adjustment to fluctuations in the external and internal world. Therefore, the proper functioning of motor systems depends on a constant influx of sensory information including information about the environment and objects around us as well as information about body position in space.

In general, two different control strategies, feedback and feedforward, have been proposed to explain how we are able to execute precise and coordinated movements to achieve goals in the surrounding environment (Wolpert & Bastian, 2021).

Feedback control refers to the process by which information about the state of the movement is used to modify the ongoing action. This information is typically provided by sensory feedback from proprioceptive, visual, and auditory sources, and is used to correct the ongoing activity in real-time. Feedback control is essential for making small adjustments to ensure that the movement is executed accurately and smoothly. For example, when typing on a keyboard, feedback control is used to ensure that each key is pressed with the right amount of force and accuracy.

In contrast, feedforward control is a process by which information about the desired outcome of the movement is used to initiate and adjust the movement before it even begins (Kawato, 1999). Feedforward control relies on prior experience and knowledge to anticipate and prepare the appropriate action before sensory feedback is available. This allows for movements to be executed rapidly and efficiently, without the need for constant sensory feedback. For example, when reaching for an object, feedforward control is used to plan and initiate the movement before the hand actually touches the object.

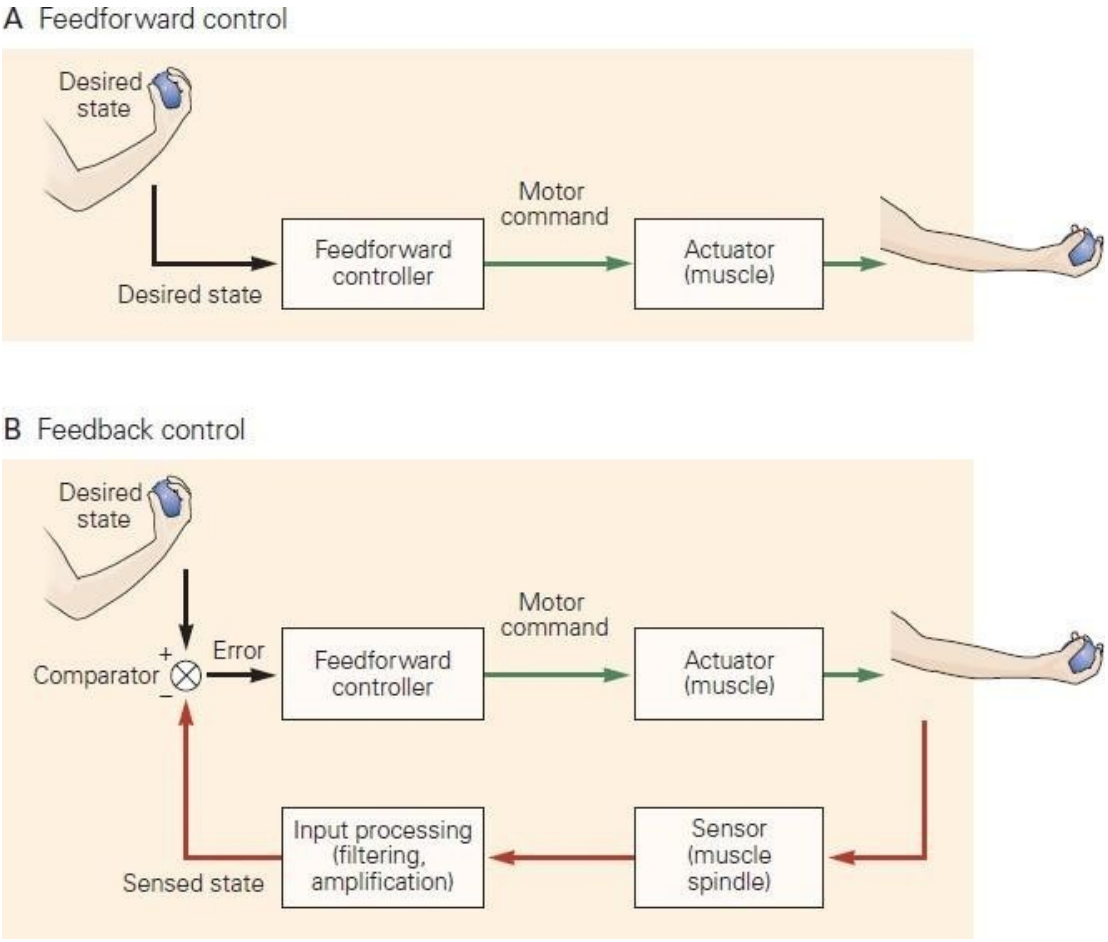

Figure 1. Feedforward and feebdack control.

A. The generation of a feedforward motor control command relies on a desired state without monitoring any potential errors that may arise during the movement.
B. Feedback control entails comparing the desired and sensed states, typically at the comparator, to produce an error signal that informs the motor command. However, there can be significant delays in the sensory feedback reaching the comparator (*from* Wolpert & Bastian, 2021).

1.1 Movement at the 'microscopic' scale

1.1.1 Movement intermittency

Human motor control theories have long sought to answer the question of how the brain can produce online motor adjustments in light of delays affecting sensorimotor control loops and inherent signal-dependent noise in the human sensory and muscular system (Harris & Wolpert, 1998). Motor control theories have pointed out the necessity of using feedforward

control with internal models to solve the challenges of producing real-time motor control (Kawato, 1999). This approach has been largely studied in the context of ballistic movements, such as rapid eye movements and rapid reaching or pointing movements, as it requires motor commands to be calculated before the movement onset with very few influences from sensory feedback. Nevertheless, feedforward control is fundamental also in continuous, time-changing, and environment-dependent motor tasks such as target tracking. Dating back to the seminal papers by Craik (Craik, 1947) and Vince (Vince, 1948), it has been proposed that feedforward control in continuous motor tasks is operated intermittently. The intermittent control hypothesis suggests that centrally integrated sensorimotor control systems act through a series of open-loop trajectories determined by intermittent feedback. According to this hypothesis, the brain divides time into discrete intervals and performs pre-programmed, serial actions in each interval, using a control strategy that can be described as *observe continuously, act intermittently* (Loram et al., 2011). In other words, internal computational processes, such as optimizing parameters, predicting, and planning motor actions, operate discreetly based on sampling internal and external events (Figure 2).

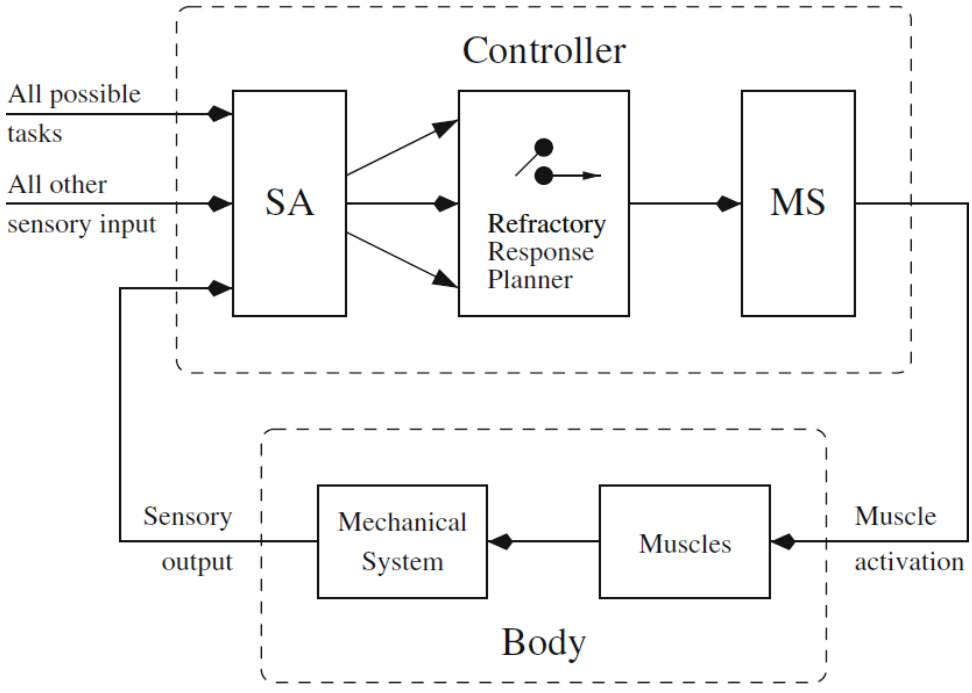

Figure 2 The Intermittent Control hypothesis explains the sensorimotor control of continuous tasks as a feedback loop where a controller uses sensory output to control muscle activation of mechanical system of the body. The controller uses sensory analysis (SA) to estimate states and the motor system (MS) to generate muscle activations. A refractory response planner intervenes between sensory analysis and the motor system, using current states to plan a trajectory of muscle activations executed without feedback. This control trajectory

is not updated until the next trajectory is planned based on updated sensory information (*from* Gawthrop et al., 2022).

The sampling of feedback and thus, of motor updating, can be either at regular intervals (clock-driven) with unresponsive periods corresponding to psychological refractory periods, or triggered by specific events, such as when the error exceeds a certain threshold (event-driven). Moreover, it has been proposed an adaptive intermittent model stating that the length of the interval is adaptively adjusted based on the prediction error and the reliability of internal models (Sakaguchi et al., 2015). Overall different studies converge in stating that intermittency is either physiological, probably arising in the central nervous system (CNS) (Van De Kamp et al., 2013), and effective in reducing the computational burden of motor planning as well as in stabilizing the control system despite the sensorimotor delays (Loram et al., 2011, 2014). Additionally intermittency subsumes, as a special case, situation in which explanation of continuous control seem more apparent because of a *masquerading effect* (Gawthrop et al., 2011).

1.1.2 Behavioural correlates of movement intermittency: submovements

The intermittent updating of motor program giving rise to the phenomenon of movement intermittency is apparent on a behavioural level in the form of small bell-shaped bumps or discontinuities, named submovements. Continuous movements indeed are never smooth but are organized into elementary units occurring approximately 2/3 times per second (2-3 Hz) that can be detected as local peaks in the kinematic profile (for an example see Figure 3). Since their first description over a century ago (Woodworth, 1899), different studies have reported the presence and the timing of submovements emission in the velocity (Miall, 1996; Tomassini et al., 2022), acceleration (Pereira et al., 2017) and force (Colomer et al., 2022) profiles in various visuo-motor tracking tasks carried out both in human and in monkeys (Susilaradeya et al., 2019). In most of these studies, experimental subjects were asked to track the continuous sinusoidal movement of a target appearing on a computer screen with a 2D cursor reflecting e.g. angular position of a manipulandum, isometric finger force. In line with the hypothesis of an event-driven intermittent control, it has been shown that the magnitude of the submovements as well the timing of their emission is influenced by tracking errors due to experimental manipulations such as visual feedback delays or spatial perturbations of the cursor relative to the target (Susilaradeya et al., 2019). These findings

suggest that submovements are corrective movements mostly driven by visual feedback and are emitted only when the observed tracking error exceeds a certain threshold. The intervals between consecutive submovements define a range of inputs, below the threshold, where the control system is unresponsive, referred to as the *error dead zone* in engineering literature (Wolpert et al., 1993). However submovements can persist even without visual feedback (Doeringer & Hogan, 1998) suggesting that they may reflect an amodal process of action planning/selection that has nothing to do with vision (Loram et al., 2014). Therefore and in accordance with the hypothesis of a clock-driven intermittent control, it has been proposed that intrinsic cyclical dynamics within motor cortical networks, giving rise to internal refractory period, might break down complex movement into sequential and elementary constituents, i.e. submovements. Recent electrophysiological findings from neural motor region show that local field potential (LFP) in monkeys (Hall et al., 2014; Susilaradeya et al., 2019) and event related potential (ERP) in humans (Pereira et al., 2017) are phase-locked and coupled to submovements frequencies, suggesting that intrinsic cortical oscillations in the delta-theta band (2-5Hz) contributes to low frequencies in motor behaviour. In the attempt to reconcile the opposing experimental findings some authors suggest that the timing of submovements emission might depend either on extrinsic, environment-dependent, visually- mediated factors and on intrinsic and cerebral-dependent factors (Susilaradeya et al., 2019).

Finally, it is worth to mentioning that different account consider submovements as *dynamic primitive* of motor behaviour stemming from functional (Hogan & Sternad, 2012) or biomechanic (Dounskaia et al., 2005) constraints. In this view, especially slower movements (more than 400 ms), are believed to be unavoidably split into discrete sequences of concatenated submovements, suggesting that they are inherent, invariant features of movement execution (Torricelli et al., 2022).

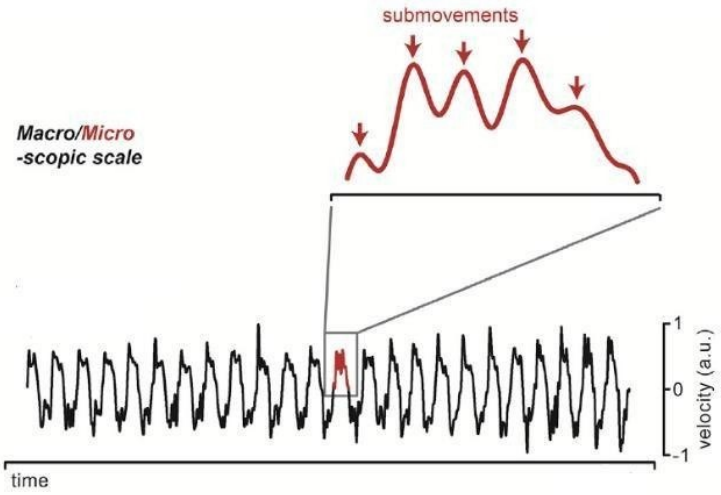

Figure 3. Zoom into the 'microscopic' scale of the movement, i.e. submovements (red trace), embedded within the 'macroscopic' scale (black trace) of the velocity profile during a visuo-motor tracking task (*Adapted from* Tomassini et al., 2022).

In conclusion, submovements play a crucial role in movement control and their presence and timing are influenced by a variety of factors, including visual feedback, intrinsic dynamics, and biomechanical constraints. Further research is needed to fully understand the underlying mechanisms of submovements in movement control, particularly in relation to their temporal dynamics. The majority of studies conducted in humans, involving continuous tracking tasks, have primarily focused on analyzing the spectral characteristics of velocity derived from a joystick (Miall et al., 1993) or isometric finger force (Susilaradeya et al., 2019). However, these studies merely acknowledge the existence of submovements within specific frequency ranges and single-handed movements, disregarding the temporal patterns of submovement generation across multiple effectors and in the context of interpersonal motor coordination.

1.1.3 Neural correlates and neurological test cases for movement intermittency

While neural correlates of movement intermittency has not yet definitively established, different studies have provided evidences of the involvement of several cortical and subcortical areas. A study, where the ongoing magnetic activity of human subjects' brain was recorded while subjects performed continuous movement of their hands, found significant coupling between hand speed and oscillatory activity in primary motor cortex and the cerebello-thalamo-cortical loop at frequencies (2-5 Hz), partly corresponding to those of submovements (Jerbi et al., 2007). Moreover supplementary motor area (SMA) and precentral gyrus were found to be coupled to submovements in a study aiming to find

electrophysiological correlates of action monitoring in continuous, visually-guided movements (Pereira et al., 2017). Finally, it has been proposed that basal ganglia and cerebellum, due to their role in action selection and online correction, respectively, might represent a potential neurophysiological basis for movement intermittency (Houk et al., 2007; Loram et al., 2014). Therefore, patients with Parkinson's disease (PD) and cerebellar disorders (CD), due to basal ganglia and cerebellum involvement in the respective pathophysiology, may serve as ideal test cases for evaluating the role of these two brain regions in movement intermittency.

1.2 Motor coordination

The vast majority of the movements we perform involve coordinating with others' movements (interpersonal coordination) or coordinating various parts of our own body (intrapersonal coordination). In the following paragraphs, I will describe these two forms of coordination and how they are achieved through different mechanisms and constraints. Understanding these mechanisms and constraints is important because they represent the motor task contexts within which I will investigate the microscale motor control mechanisms underlying movement coordination.

1.2.1 Bimanual coordination

Many daily activities involve coordinating individual actions and, more specifically, cooperation between the hands (bimanual coordination). The evolution of primates towards upright standing has freed the hands for manipulating objects and performing complex actions, such as making food and playing musical instruments. Some tasks require synchronous coordination of both hands, such as lifting objects, while other tasks involve a differentiated role, with one hand performing the main action and the other serving as a stabilizer, such as opening a bottle (Swinnen & Wenderoth, 2004). Bimanual coordination has gained substantial attention in recent years and provides a starting point for exploring higher cognitive functions, including executive abilities like task switching, multitasking, and inhibition. Additionally, it serves as a foundation for investigating lateralization and asymmetry processes, as well as the connection between brain structure and behaviour, with a focus on the corpus callosum (CC) (Gooijers & Swinnen, 2014). The principles and constraints underlying bimanual control have been widely investigated from two different

theoretical viewpoints. The information-processing perspective views bimanual coordination as a type of dual-task performance that is affected by mutual interference, i.e., neural cross talk, resulting from the simultaneous tasks carried out by each limb due to restricted neural resources. In particular, this form of interference has been studied when the subtasks performed by each limb differ in timing, amplitude, force, or direction (Cattaert et al., 1999; Sherwood, 1994). Within the dynamical system perspective, bimanual coordination patterns have been regarded as self-organizing and emergent properties resulting from the interaction of different subcomponents at multiple levels, from neural to musculoskeletal (Bressler & Kelso, 2001; Kelso, 1995). In particular, two patterns seem to act as attractors constraining the way bimanual movements are coordinated and preferentially executed: the in-phase mode ($\Phi = 0°$) and the anti-phase mode ($\Phi = 180°$), consisting in the simultaneous activation of homologous and non-homologous muscles, respectively (Kelso, 1995). In-phase and anti-phase coordination modes are observed more frequently than any other phase relationships, especially at low frequencies, and are typically replicated across different effectors during daily activities. The stability of these coordination patterns relative to different phase relationships (e.g., $\Phi = 90°$ or 135°) between limbs, can also result from the performer's tendency to favor simple time intervals due to limitations in perceiving and producing complex temporal relationships (Semjen & Ivry, 2001). In this respect, bimanual coordination seems to be affected also by temporal constraints (Figure 4) that reflect the preference of the central nervous system to encode the movement of different effectors within a common time frame. For example, executing simple rhythms (1:1, 2:1) that involve one limb moving at an integer multiple of the other limb is simpler than performing more complex polyrhythms (3:2, 5:3) (Summers et al., 1993). Finally, amplitude and directionality have been recognized as two spatial constraints affecting complex bimanual movements. The default mode is to produce movements with the same amplitudes and directionality, as evident from the assimilation effects when executing two movements simultaneously at different amplitudes or in different directions. This is especially evident when drawing lines with different directions simultaneously or combining line and circle drawings, where is possible to observe the progressive tendency of the two limbs to move at the same amplitude or towards the same direction (Franz et al., 1996; Sherwood, 1994).

Overall, bimanual coordination is achieved through the interplay of constraints at various levels of the motor system: some being closely tied to the neuromuscular output system, i.e. to the relative timing of muscles activation, others being more associated with abstract neural codes, i.e. specification of temporal and spatial features. Although coordination constraints

can pose difficulties for individuals, they can be overcome, as demonstrated by daily activities such as driving that necessitate distinct patterns of limb activation patterns. In some cases, overcoming these constraints may come easily but in others, it may require a lot of practice, as can be seen in expert athletes, dancers, or musicians. The goal of motor learning is to overcome fundamental coordination constraints causing persistent performance errors and to promote the exploration of less favoured coordination modes. Different strategies have been proposed for enriching the bimanual coordination repertoire beyond the limitations imposed by constraints. For example, abstract binding rules, supporting the integration of the subtasks into a common temporal structure, or visual transformation simplifying the representation of the task being performed (Swinnen & Gooijers, 2015).

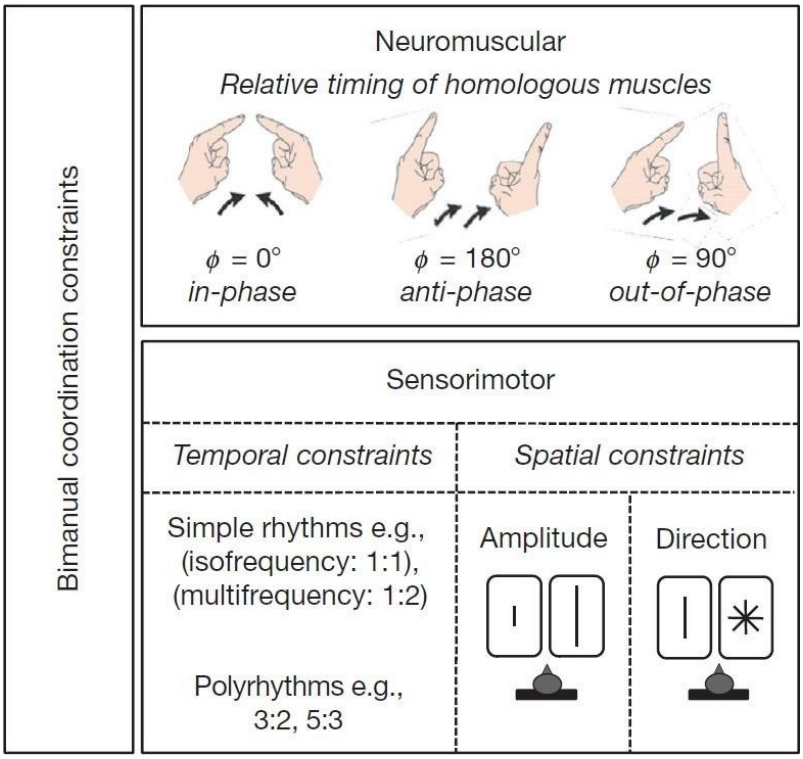

Figure 4. Overview of neuromuscular and sensorimotor constraints affecting bimanual coordination (*from* Swinnen & Gooijers, 2015).

Different brain regions, including primary motor cortex (M1), premotor and supplementary motor areas and cerebellum, are involved in bimanual coordination tasks (Swinnen & Wenderoth, 2004). Prefrontal, parieto-occipital, temporal areas and the insular cortex may also be activated depending on internal factors (such as expertise level, age, and pathology), as well as external factors (task difficulty and complexity). Finally, recent research has highlighted the relevance of the corpus callosum (CC) in bimanual coordination through studies conducted on split-brain patients and those with agenesis of the CC (Eliassen et al.,

2000). Although these patients can effectively execute familiar activities like tying their shoes, they struggle to acquire new skills, emphasizing the critical function of the CC in exchanging sensory information between both limbs to successfully integrate goal-directed tasks (Franz et al., 2000; Gooijers & Swinnen, 2014).

1.2.1 Interpersonal motor coordination

Interpersonal coordination involves synchronized and patterned actions between individuals in social interactions, consisting of behaviour matching and interactional synchrony (Bernieri & Rosenthal, 1991). Behaviour matching is closely related to imitation, while interactional synchrony refers to the alignment of one's behaviour with the timing and movements of the interacting partner through alternating cycles of engagement and disengagement (Condon & Ogston, 1967). Interpersonal coordination has been widely acknowledged as a crucial factor in promoting prosocial behaviours, serving as a "social glue" that fosters social interactions. Interpersonal coordination has been shown to promote cooperation, sharing, trust, closeness, improved perception of others, and to play a key role in the development of empathy, social understanding, and affective regulation (Valdesolo et al., 2010; Miles et al., 2010; Launay et al., 2013; Tarr et al., 2016; Rabinowitch & Meltzoff, 2017). Interpersonal synchronization can arise both intentionally and unintentionally in social contexts. Unintentional forms of synchronization encompass limb movement alignment (Schmidt et al., 1990), gesture matching during communication (Louwerse et al., 2012), and synchronized hand clapping at concerts (Néda et al., 2000). In contrast, intentional synchronization is guided by top-down control, such as in the case of marching soldiers or playing musicians (Keller et al., 2014). Research has explored spontaneous behavioural synchronization in activities such as drumming (Kokal et al., 2011), eye movement (Richardson et al., 2005), and body posture sway (Shockley et al., 2007). Other studies have instructed participants to synchronize movements with a partner (e.g. walking, rocking chair; Richardson et al., 2007; van Ulzen et al., 2008) or to move in sync with a rhythmic stimulus (Lakens & Stel, 2011; Valdesolo & DeSteno, 2011).

To coordinate effectively, interacting partners need to comprehend and anticipate each other's actions (Sebanz & Knoblich, 2009). Indeed, effective joint action relies on the abilities of the interacting partners "(i) to share representations, (ii) to predict actions, and (iii) to integrate predicted effects of own and others' actions" (p.70, Sebanz et al., 2006).

Research suggests that anticipatory mechanisms facilitate rhythmic interpersonal coordination by using forward models that simulate the production of one's and others'

actions slightly in advance (Sänger et al., 2011). In particular, the combination of an individual's forward model and their interaction partner's forward model into a "joint" forward model enables smooth interpersonal coordination by predicting and correcting any potential timing errors before they occur (Vesper et al., 2017). According to Müller et al. (2021), the forward model of joint action consists of three layers, each representing the individual's own forward model, their interaction partner's forward model, and a representation of the shared or joint forward model, respectively (Müller et al., 2021). As per this model, in the first layer, the individual creates an action intention and prediction based on the joint goal and external influences. The sensorimotor system integrates this information and implements the motor command, sending an efference copy to compare with the sensory consequences of action execution. The comparison between the predicted and actual outcomes informs subsequent actions and helps in achieving the joint goal. The second layer, corresponding to the representation of other's forward model, reflect the individual capability, based on motor simulation, to predict the consequences of the interacting partner's action. The consideration and integration of the other's action intention and prediction provides information on the expected and actual sensory consequences of other's actions. Comparing these predictions with actual outcomes can help individuals align their actions with those of their partner. Finally, in the third layer, the joint action intentions and predictions are integrated to generate information about the expected and actual sensory outcomes of joint action. The comparison between the predicted and actual joint action outcome can facilitate improved coordination among individuals. The outcome of this comparison between expected and actual sensory consequences, which takes place across all three representational layers, determines the ending of the forward model - either through the achievement of the joint goal or through correction to ensure goal attainment.

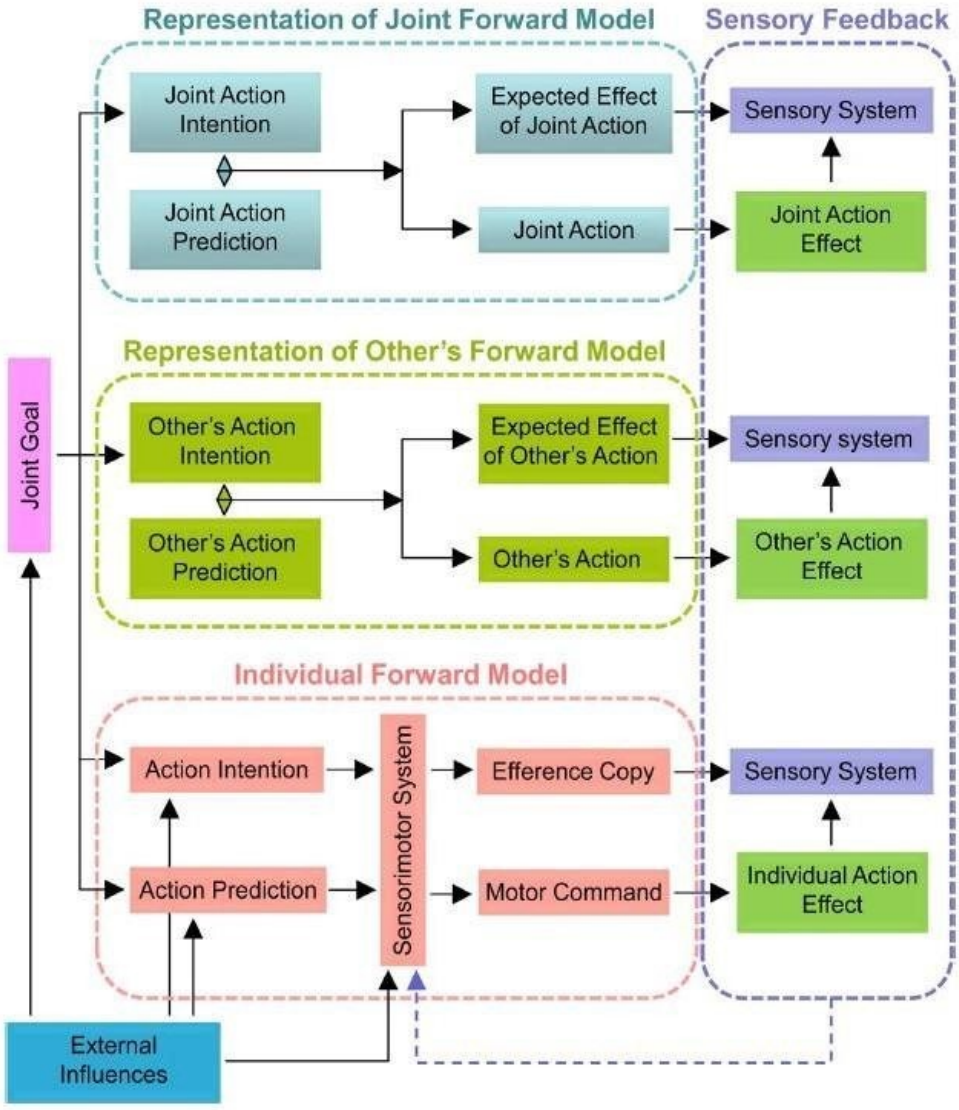

Figure 5. Graphical representation of the three-layered Forward Model of Interpersonal Motor Coordination.

In the first layer, the individual generates an action intention and prediction based on external influences and a joint goal. The second layer involves the other person's forward model representation, which includes their action intention and prediction, as well as the expected sensory outcomes. The third layer represents the joint forward model, including the joint intention and prediction, which is compared to the actual outcome of the joint action. Sensorimotor feedback loops intertwine the different representational layers, where the intended and predicted action are compared, thus determining the progress of coordinated action (*from* Müller et al., 2021).

Synchronization of brain activity is essential for coordinating actions with others and is a key aspect of neuronal and sensorimotor communication both within and between individuals (Pezzulo et al., 2019). EEG hyperscanning studies provide evidence that brain oscillations synchronize within and between the brains when people engage in different forms of action coordination. Overall, these studies indicate that interpersonal action coordination is associated with neuronal coupling primarily in the frontal and centro-parietal

regions, with a predominance in lower frequency bands (Czeszumski et al., 2020). However, the frequency bands associated with movement synchronization are still unclear. Some studies found predominant effects in the alpha (10–12 Hz) and beta (~ 20 Hz) frequency ranges, while others exclusively emphasized synchronization in the theta frequency (3-8 Hz) excluding the alpha range (Lindenberger et al., 2009; Dumas et al., 2010; Novembre et al., 2016). Indeed, it is thought that an increase in theta activity in the occipito-temporal regions contributes to the integration of visual and motor information during interaction (Era et al., 2019).

Introduction to experimental section

The studies presented in the following chapters are not organized chronologically. Instead, they follow a theoretical gradient based on the level of complexity and from intra-personal coordination to inter-personal coordination (i.e., from bimanual to interpersonal coordination). I will begin withthe first study, which involves a bimanual coordination task performed by single subjects. Next, I will move onto the second study, in which two subjects engage in a unimanual coordination task. The third study is a combination of the first two, where pairs of interacting subjects are asked to perform a coordination task using both their hands. Study 4, is a unimanual task performed with a virtual partner. Study 5 extends and adapts the set-up of Study 4 to a clinical population and specifically on subjects with Parkinson's disease and cerebellar disorders. As I mentioned earlier, this sequence of studies follows a logical order rather than a purely chronological one. In fact, Study 2 and Study 4 has already been published (Tomassini et al., 2022), while I'm now finalizing the write- up of Study 1 and 3 for submission. Study 5 is still running due to the significant new challenges posed by the analyses of patient kinematic data. Due to this reorganization based on a conceptual ground, the reader will see that studies that were published first (i.e., Studies 2 and 4) are corroborated by a number of complementary analyses and controls. Building on this foundation, laterstudies limited the analyses to the time domain only because they were considered more informative for analysing the phenomenon in question.

Chapter 2

2.1 Study 1. *Intra-personal motor coordination goal: Bimanual Task.*

2.1.1 Abstract

In this study, we analysed the temporal relationship between submovements emitted by a single participant's hands during a bimanual coordination task. We also manipulated the availability of visual feedback to understand how it affects the emission of submovements. Time-domain analysis was performed on the kinematics data of both index fingers, which were recorded by a motion-capture system. Our analysis revealed a complex pattern of alternating and simultaneous emission of submovements between the fingertips of both hands during the open-eyes condition, whereas a quasi-simultaneous pattern of submovements emission was observed during the closed-eyes condition. Overall, the results suggest a different role of visual and proprioceptive feedback in modulating submovements emission.

2.1.2 Personal contribution

I implemented the experiment, recorded the data and performed all the analyses using codes I wrote in Matlab under the supervision of Dr. Alice Tomassini and Prof. Alessandro D'Ausilio. In the near future we plan to write a paper about the data herein presented.

2.1.3 Sample

Thirteen participants (6 females and 7 males, age: 24.85 ±5.24 years) were recruited for this study. All participants had normal or corrected to normal vision and they self-reported being

right-handed. This was also verified by the experimenter who checked the handedness of the participants while they filled out ethics forms before the experiment.

2.1.4 Procedure

Participants were asked to sit at a table with the ulnar sides of their left and right forearms resting on the surface. They were instructed to hold their hands in a closed fist posture, with only their left and right index fingers pointing towards each other (the distance between the participant's left and right index fingers was approximately 1.5 cm; Figure 6A). Participants were asked to perform rhythmic (15 beat per minute, bpm, pace) flexion-extension movements, as synchronously as possible, either in-phase or anti-phase, once with their eyes open and once with their eyes closed (Figure 6B). In the Closed Eyes Conditions, participants were asked to maintain the same gaze direction they had during the Eyes Open Condition, as if they were observing their own index finger movements. In the In-phase Conditions, participants were instructed to perform an extension movement as first movement for both index fingers, whereas in the Anti-phase Condition, they were instructed to perform a flexion movement for the right index finger and an extension movement for the left index finger as first movement (Figure 6B). Participants familiarized themselves with the requested pace by listening to a metronome prior to the experiment. The metronome was silenced during the trials and briefly replayed at the start of each condition. The order of the conditions was randomized for each participant. Overall, participants performed eight trials (two for each different condition: in-phase vs. anti-phase and open vs. closed eyes) for a total duration of approximately 25 minutes.

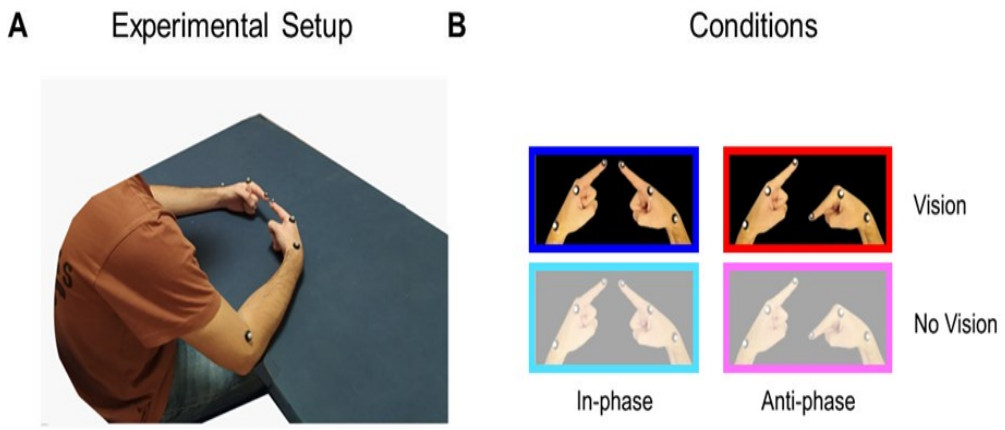

Figure 6. Experimental Setup and Procedure

A. We asked participants to sit at a table and rest the ulnar sides of their left and right forearms on the surface

while making a closed fist with their hands and positioning their left and right index fingers pointing towards each other.

B. We asked participants to perform rhythmic flexion-extension movements at a 15 bpm pace, as synchronously as possible, either in-phase or anti-phase., once with their eyes open and once with their eyes closed. We manipulated two factors: Movement (In-phase vs. Anti-phase) and Vision (Open Eyes vs. Closed Eyes).

2.1.5 Kinematic data recording

We recorded the kinematics of movements using a ten-camera motion capture system (Vicon Nexus, with a sampling rate of 300 Hz) along three axes: mediolateral (X), anteroposterior (Y), and vertical (Z). However, we limited our analysis to the main anteroposterior movement axis (Y-axis). To collect position data, we placed retro-reflective markers on the distal phalanxes of the right and left index fingers (marker diameter: 6.4 mm). Figure 6A shows two additional markers placed on the metacarpophalangeal joint (marker diameter: 9.5 mm) and the styloid process of the radius (marker diameter: 9.5 mm) of both hands for reconstruction purposes. An additional marker was placed on the right lateral epicondyle of the humerus to differentiate between the right and left hands.

2.1.6 Time Domain Analysis

Analyses were performed with custom-made codes programmed within MATLAB computing environment while the data were filtered using FieldTrip Toolbox.

Segmentation and pre-processing of velocity data

The onset of each flexion/extension movement was identified on low-pass filtered (3 Hz, two-pass Butterworth, third order) position data. The movement onsets were defined as peaks in position data that corresponded to the inversion of movement direction: from flexion to extension and vice versa. Peaks were detected on position data whose sign was adjusted to be positive in all recorded trials. Thus, we circumvented the negative signs of flexion movements with respect to the main axis of the movement. The identified movement onsets were then visually checked on both position data and on corresponding velocity data. In the latter case, we ascertained that the peaks detected in position data coincided with the samples where the velocity passed through zero. All errors in data segmentation were

manually corrected: Segments in which participants lost the coordination mode with the index finger of their other hand were removed from the analysis. Likewise, all segments with durations greater than or less than 2.5 standard deviations from the mean movement duration (computed trial-wise on all retained segments of single participants' index fingers) were excluded from further analysis.

Finally, the time stamps of the movement onset were then used to segment the velocity data, which was computed as the first derivative of the position data low-pass filtered at 4 Hz (two-pass Butterworth filter, third order). All the analysis were performed on velocity data pre-processed as follow:

1. The sign of the velocity segments was changed to ensure that all velocity segments were positive (first step: change of velocity sign).
2. The velocity was normalized based on the maximal speed calculated trial-wise for each index finger (second step: velocity normalization).
3. The average velocity profile was subtracted from each index finger to remove movement-related components (third step: average velocity profile subtraction).

Temporal characterization of movements at macroscopic and microscopic scales

To analyse the temporal synchronization at the macroscopic level of the movement (Movement Synchronization; Figure 7A), we first calculated the mean and standard deviation of the absolute differences in movement onsets between the right and left index fingers of each participant. Next, we calculated the grand average of these means and standard deviations across all participants for each condition. At the microscopic level, we evaluated the mean and variability of submovements emission to measure the timing between submovements (Inter-submovements Time; Figure 7B). To this end, we identified submovements as local peaks in the velocity segments of each individual participant's right and left index fingers. We then calculated the mean and standard deviation of the differences in submovements onset (trial-wise), taking into account both index fingers of each participant. Finally, we calculated the grand average of the means and standard deviations of inter-submovements onsets across all participants, for each condition.

Submovement-locked analysis (qualitative analysis) and Submovement-locked probabilities (quantitative analysis)

For the submovement-locked analysis (qualitative analysis, Figures 8A and 8B upper panels), we detected the submovements as local peaks in velocity segments of participants'

right index fingers. We then segmented the velocity segments of the right and corresponding left index finger within a time window of ±0.6 seconds, centred around the identified submovements in the right hand. Importantly, the velocity segments of the left index finger were preliminarily time-aligned with the movement onsets of the right index finger to restore the actual temporal relationship between the movements of both hands as they occurred during the experiment. The velocity segments of the left index finger, which were time-aligned to the submovements of the right index finger, were also used to compute the probabilities of emitting submovements based on those emitted by participants' right hand (quantitative analysis, Figures 8A and 8B lower panels). This probability was estimated by counting the number of submovements identified as local peaks in the velocity segments of the left index finger for each time point, ranging from -0.6 sec to +0.6 sec relative to the submovements detected in the right index finger. The sum of submovements detected in each time point was then divided by the total number of velocity segments based on the identified submovements in the right index finger. Finally, the left hand probability of emitting a submovement at each time point was expressed as a percentage deviation from the mean probability of submovement emission computed across the entire segment duration, by summing the probability associated with each time point. The computed probabilities were then averaged within 36 non-overlapping equally spaced bins in each trial. For statistical comparison purposes, we also derived probabilities from surrogate data (quantitative analysis, see Figures 8A and 8B). The shuffling procedure was implemented through an iterative (5000 iterations) random assignment of velocity segments of the left index finger to velocity segments of the right index finger, in order to destroy the actual sequencing of movements as they were emitted during the trial. The estimation of the probability and the definition of binned probabilities for surrogate data were identical to the procedure described for the quantification of the probabilities of the original data.

2.1.7 Statistical Analysis

Comparison of movements at macroscopic (Movement Synchronization) and microscopic (Inter-submovements Time) scales

We applied a two-way repeated measure ANOVA to test whether there were significant differences across conditions in both the Movement Synchronization and the Inter-submovements Time levels (Figure 7).

Original binned time-locked probabilities vs. surrogate binned probabilities

We performed a two-tailed t-test that was Bonferroni-corrected for the number of bins considered ($p < 0.0014$) to assess whether there were statistically significant differences in mean probabilities calculated from the original and surrogate data within each of the 36 temporal bins.

2.1.8 Results

The participants were able to synchronize the movements of their right and left index fingers significantly better during in-phase than anti-phase conditions (principal effect of movement: $F_{1,12}$= 9.208, p = 0.01) and also when they had access to visual feedback (principal effect of vision: $F_{1,12}$= 13.736, p = 0.003). Furthermore, they showed less variability in producing quasi-simultaneous movements between their hands when visual feedback was available (principal effect of vision $F_{1,12}$= 10.716, p = 0.007). However, there were no significant movement * vision interactions for either the means ($F_{1,12}$= 0.068, p =0.798) or standard deviations ($F_{1,12}$= 0.037, p =0.85) of the absolute differences in movement onsets (Figure 7A). At the Inter-submovements Time level, the movement had significant principal effects on both submovements emission ($F_{1,12}$= 11.77, p = 0.005) and variability ($F_{1,12}$= 18.49, p= 0.001) of their emission, while vision had a significant principal effect only on the variability of submovements emission ($F_{1,12}$= 15.179, p= 0.002). No significant movement*vision interactions were found for either the means ($F_{1,12}$= 1.051, p =0.326) or standard deviations ($F_{1,12}$= 0.919, p =0.357) of the differences in submovements production (Figure 7B).

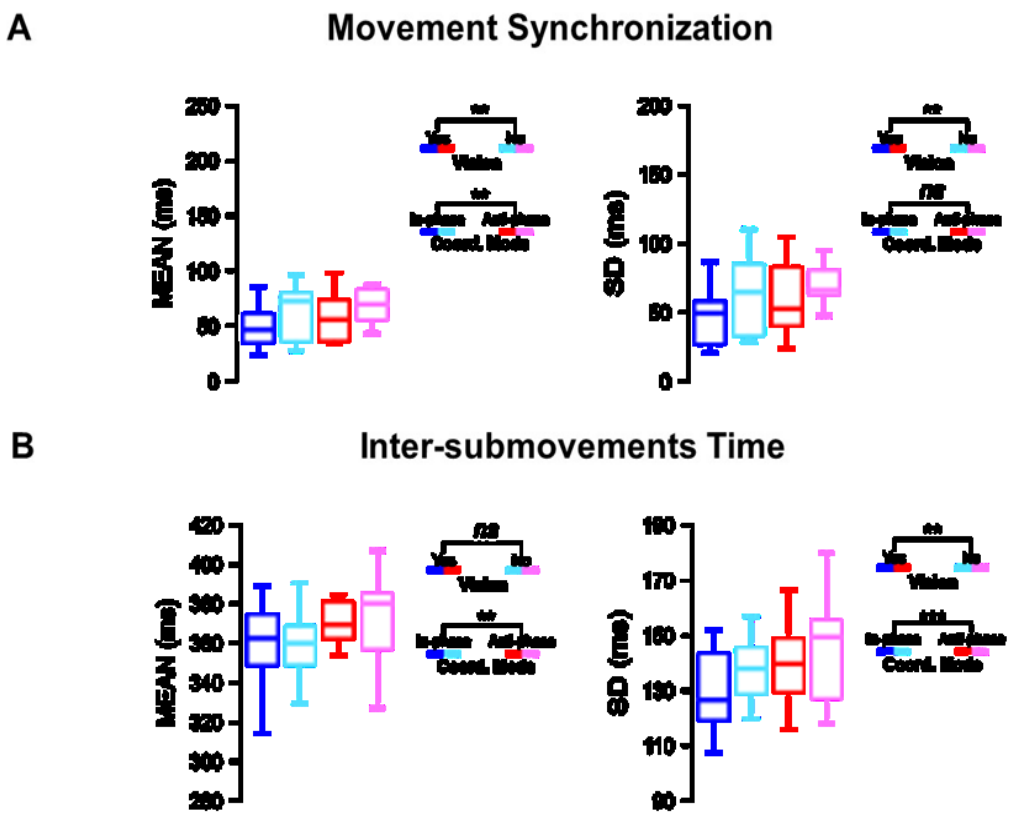

Figure 7. Temporal characterization of movements at macroscopic and microscopic scales

A. Mean and standard deviation of the absolute differences in movement onsets between participants' index fingers computed across subjects for each condition.

B. Mean and standard deviation of the differences in submovements onset, detected as local peaks in the velocity segments of single participant's right and left index fingers, computed across subjects for each condition.

*$p \leq 0.05$
**$p \leq 0.01$
***$p \leq 0.001$

Looking at the temporal relationship between submovements of the two hands, we found that in the absence of visual feedback, a quasi-simultaneous relationship occurs between left and right index finger submovements, regardless of whether the coordination mode is in-phase or anti-phase (see Figure 8B). The co-occurrent relationship is confirmed quantitatively by comparing original probabilities vs. surrogate probabilities of the left index finger to emit a submovement given the one produced by the right index finger. A one-tailed t-test, Bonferroni-corrected for multiple comparisons, reveals a significant difference precisely at the time when a submovement is emitted by the right index finger. However, when visual feedback is available, the temporal relationship of submovements is more complex, potentially indicating a mixed relationship of anticipation and simultaneity between submovements of the two hands. At a qualitative level, submovements emitted by

the left index finger during the In-phase Open Eyes condition (Figure 8A, upper panel on the left) appear to occur over a wider temporal window around the submovements emitted by the right index finger, with a stronger tendency to anticipate them. The original probability of submovements emission (vs. surrogate probabilities) is significantly different exactly at the time when the right index finger submovement is emitted, as well as in temporal windows preceding the right index finger submovement. The mixed relationship of anticipation and simultaneity is also apparent in the Anti-Phase Open Eyes condition, although it is less clear at the qualitative level. Indeed, the original vs. the surrogate probabilities of emitting a submovement are significantly different in temporal ranges both preceding and occurring simultaneously with the moment when a submovement is emitted by the right index finger.

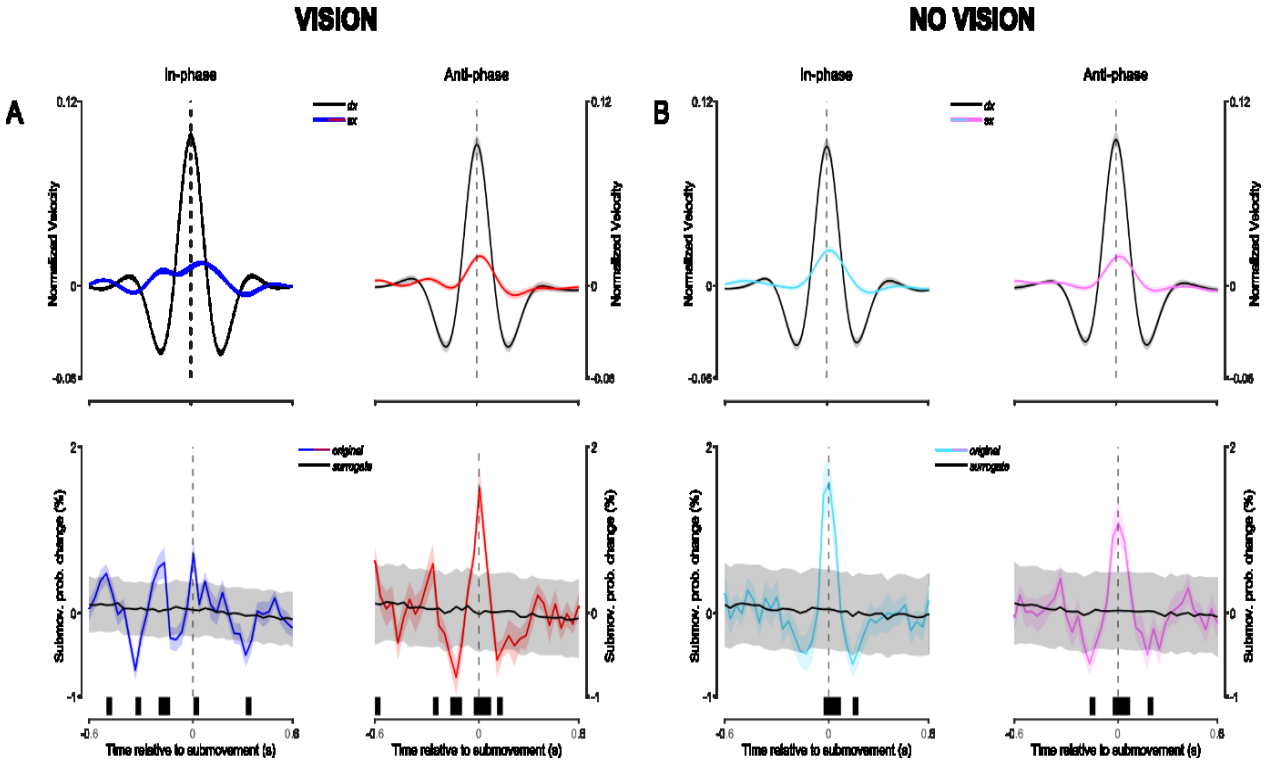

Figure 8. Temporal dynamics of submovements modulation

Upper Panels 8A-8B. Velocity of both left and right index fingers locked to submovements generated by the right index finger (mean ± SEM).

Lower Panels 8A-8B. Submovement probability (expressed as deviation from mean probability) for left index as a function of the actual time (original time-aligned data) or of random assigned velocity segments (surrogate data) from submovements generated by right index finger. The black bars indicate the time points that survive two-tailed t-test statistics on time-aligned original data vs. surrogate data (Bonferroni-corrected for multiple comparisons across time).

Chapter 3

3.1 Study 2 *Inter-personal motor coordination goal: Unimanual Task.*

3.1.1 Abstract

In this study, we aimed to extend beyond examining the temporal emission of submovements in single individuals by exploring their dynamics during interpersonal coordination. We performed frequency-domain and time-domain analyses on the kinematics of the index fingers of two interacting participants, recorded using a motion-capture system. Our analyses revealed that the submovements of the two partners alternate over time during in-phase coordination, suggesting a mutual adaptation of participants' submovements during social interaction

3.1.2 Personal contribution

The text and figures presented below are retrieved from the already published paper *Tomassini, A., Laroche, J., Emanuele, M., Nazzaro, G., Petrone, N., Fadiga, L., &D'Ausilio, A. (2022). Interpersonal synchronization of movement intermittency. Iscience, 25(4), 104096* (https://doi.org/10.1016/j.isci.2022.104096) in which I was involved in data collection and I had the opportunity to learn how to apply most of the analyses that I then used in the other studies.

3.1.3 Sample

Eighty participants (40 females) formed 40 gender-matched couples. Thirty couples (age 23.9 ± 4 years, mean ± SD) took part to the main experiment and 10 couples (age 26.2 ± 4 years) participated in the control experiment. Except two authors (A.T. and G.N.), participants were all naïve with respect to the aims of the study and were paid (€ 12.5) for their participation. All participants were right-handed (by self-report) and had normal or

corrected-to-normal vision. The study and experimental procedures were approved by the local ethics committee. Participants provided written, informed consent after explanation of the task and experimental procedures, in accordance with the guidelines of the local ethics committee and the Declaration of Helsinki.

3.1.4 Procedure

All couples participating in the main experiment (n = 30) performed the same primary task ('Real partner') and a subsample of couples (n = 20) performed also one of two different secondary tasks (randomly assigned). Task details are described in the following.

Primary task – real partner

Participants were seated at a table either alone or in front of each other (~1 m apart) with their faces hidden from view by means of an interposed panel (Figure 9A). They were asked to keep the ulnar side of the right forearm resting on a rigid support and perform rhythmic flexion-extension movements of the index finger about the metacarpophalangeal joint (Figures 9A and 9B). Movements were performed by each participant alone (solo condition) and by the two participants together (dyadic condition). In the latter condition, participants were required to keep their index fingers pointing straight towards each other (without touching) and move as synchronously as possible either in-phase (towards the same direction) or anti-phase (towards opposite directions, Figure 9B). Given the mirror-like participants' arrangement and hand posture, in-phase coordination required them to perform simultaneously different movements (i.e., as one participant performed finger flexion, the other performed extension and vice versa). Conversely, anti-phase coordination required the two participants to perform the same type of movement (either flexion or extension; see Figure 9B). In all conditions (solo, dyad-in-phase, dyad-anti-phase), participants were instructed to keep their movement rate around 0.25 Hz (15 bpm; flexion-extension cycle: 4 s; flexion/extension movement duration: 2 s). Before the experiment, they familiarized themselves with the reference rate by listening to a metronome and synchronizing their movements to the auditory beat for a short time (~1 min). Metronome was also played prior to each experimental condition for a few seconds; during the kinematic recordings the metronome was silenced, and movements were thus self-paced.

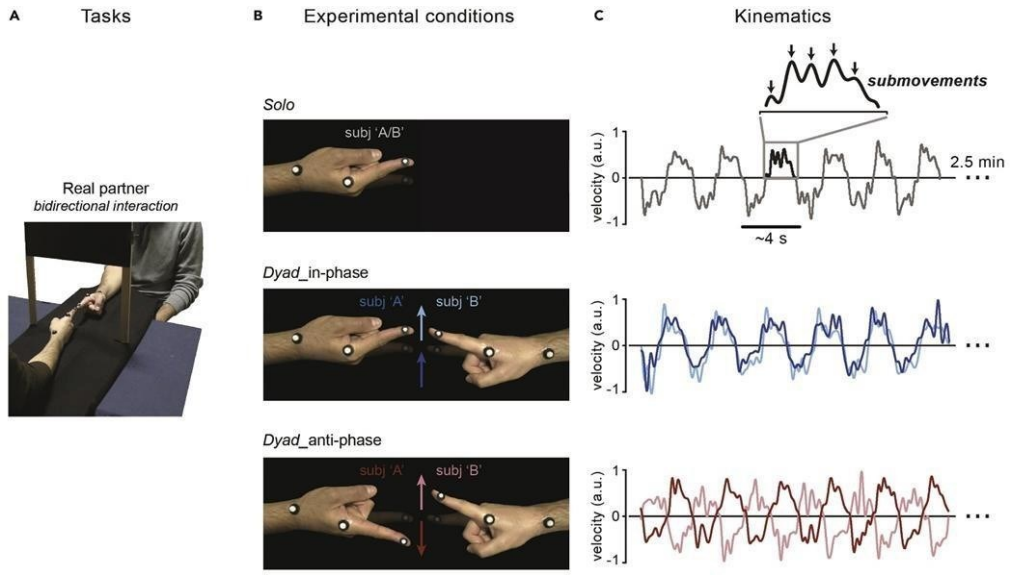

Figure 9. Experimental Setup and Procedure

A. Tasks. Primary task (‘‘Real partner’’) (for the other tasks, see Figure S2, supplementary materials). Participants seated at a table with the ulnar side of the right forearm resting on a rigid support and performed rhythmic (0.25 Hz) flexion-extension movements of the index finger about the metacarpophalangeal joint. In the primary task, participants formed couples (n = 30) and were asked to synchronize their movements to one another.

B. Conditions. Finger movements were performed by each participant alone (solo condition; top panel) as well as together with the real partner (dyadic condition; the middle and bottom panels illustrate the ‘‘Real partner’’ task). In the dyadic condition, participants were required to keep their fingers pointing straight ahead without touching each other (or the screen) and move as synchronously as possible either in-phase (toward the same direction; middle panel) or anti-phase (toward opposite directions; bottom panel).

C. Kinematics. Movements were recorded in trials of 2.5 min (two trials per condition) using a real-time 3D motion capture system (Vicon; sampling rate: 300 Hz). Examples of the participants’ finger velocity along the main movement (x-)axis, measured at the distal phalanx of the index finger (see markers in Figure 4A), are shown for all conditions. Periodic (2–3 Hz) submovements are highlighted in the inset.

Secondary tasks

Ten couples completed a second task (Real partner – Hand prone) that was similar to the primary one, except that they kept their right hand in a prone posture and moved the index finger along the vertical rather than horizontal axis (Figure S2A, supplementary materials). As opposed to the main task, during in-phase coordination the two participants had now to perform simultaneously the same type of movement (either flexion or extension), while during anti-phase coordination they had to perform different movements (as one performed

flexion, the other performed extension and vice versa). Other 10 couples completed a secondary task (Real partner – Arm) involving movement of the whole forearm, primarily around the elbow joint (Figure S2B, supplementary materials). Arm movements were performed (trial-wise) along either the horizontal or vertical inner dimensions of the window (~40 x 40 cm) delimited by the interposed panel. Only two conditions were tested: participants moved alone (solo) or tracked each other's movement by keeping the respective fingertips spatially aligned (dyad-in-phase; dyad-anti-phase was not tested in this task). Given the larger movement amplitude, the instructed movement rate was reduced to 10 bpm (i.e., ~0.17 Hz).

Control experiment – speed dependency

Couples (n = 10) completed the 'Real partner' primary task (in-phase coordination mode only) at different movement paces, including the same pace as tested in the main experiment (i.e., 0.25 Hz) and two additional paces of 0.5 and 0.75 Hz. Five couples of the same sample were additionally tested at a faster movement pace of 1 Hz.

3.1.5 Kinematic data recording

Movements were recorded along three axes (mediolateral, X; anteroposterior, Y; and vertical, Z) using a ten cameras motion capture system (Vicon; Nexus; sampling rate: 300 Hz). Three retro- reflective markers were placed at the following anatomical locations of the right hand: on the distal phalanx of the index finger (marker diameter: 6.4 mm), on the metacarpophalangeal joint (marker diameter: 9.5 mm) and on the styloid process of the radius (marker diameter: 9.5 mm; see Figure 9B).

3.1.6 Data collection

Each couple completed the whole experiment in ~1.5 h. For all tasks, data were collected in separate trials with short pauses in-between trials. Two trials of 2.5 min each were recorded for each couple and condition (solo, dyad-in-phase/anti-phase) in all tasks except the 'Arm' control task (vertical and horizontal) for which three trials of 1.5 min were recorded for each condition (solo, dyad-in-phase). The two/three trials per condition were always performed in succession. Instructions about task/condition were provided verbally before each trial sequence. Tasks and conditions order were randomized across couples.

3.1.7 Quantification and Statistical Analysis

Analyses were performed within the MATLAB computing environment using custom-made code and the FieldTrip toolbox. Analysed data corresponds to position data along the main movement axis for the marker attached on the fingertip. Velocity has been computed as the first derivative of position and normalized (trial-wise) on maximal speed.

3.1.7.1 Spectral analysis

Spectral content

Spectral analysis was performed by band-pass filtering (FIR filter, order: 3 cycles, two-pass) the continuous (2.5 min) velocity time series applying a sliding window along the frequency axis (range: 0.1–20 Hz) in 100 steps and bandwidths (range: 0.01–3 Hz) that were logarithmically (log10) spaced. Frequency-resolved instantaneous power was derived by means of the Hilbert transform and then averaged over time points (from 5 to 145 s) and trials (Figure 10).

Between-subjects phase-locking value (PLV)

The between-subjects phase-locking value (PLV) was computed as the mean resultant vector of the instantaneous phase differences (Hilbert-derived) between the two partners' velocity time series (the resulting PLV was then averaged across trials). The (between-subjects) PLV was also computed across shorter 2-s data segments (from all trials) that were time-locked to each partner's individual movement onsets (see below for details on the algorithm used to identify movement onset time). The resulting PLV was then averaged across time points (Figure S1, supplementary materials). To avoid edge artefacts, data segmentation was performed on the already band-passed filtered and Hilbert-transformed signals.

Within-subject phase-locking value (PLV)

Further, to evaluate whether submovements are phase-locked to movement onset, we quantified the within-subject (or inter-movement) PLV on the same data segments as described for the between-subjects PLV but computing the mean resultant vector over the same-participant instantaneous phases (instead of the between-participants phase differences; Figure S1, supplementary materials).

3.1.7.2 Time-domain Analysis

Detection of individual movements

To estimate onset/offset of each individual movement, we low pass filtered (3 Hz, two-pass Butterworth, third order) the position data before computing the velocity. Movement onset was defined as the first data sample of a segment equal to 1/4 of the instructed movement duration (0.5 s for the main experiment) where the velocity was positive (or negative, depending on movement direction); movement offset was defined as the first sample after at least half the instructed movement duration (1 s for the main experiment; exact time could be slightly changed according to individual movement duration) from movement onset where the velocity passed through zero. This algorithm was applied iteratively by sliding along the entire velocity time series. Data segmentation was visually checked for each time series and any error was manually corrected (<5%).

Cross-correlation

The cross-correlation analysis was performed on velocity as obtained by taking the first derivative of position data that were low-pass filtered at 40 Hz to remove high-frequency noise. For each couple and condition, we first took velocity segments corresponding approximately to individual movements, i.e., time-locked to the participant-specific movement onsets and with length equal to mean movement duration (velocity segments belonging to movements with duration > or < than mean duration ± 2.5 SD were discarded from the analysis). Velocity sign was adjusted to be positive in all segments. To remove the movement-locked components, we subtracted from each segment the average velocity profile across all the retained segments (subject-wise). After these common preprocessing steps, we computed the cross-correlation (normalized so that the autocorrelations at zero lag are identically 1) by aligning the two partners' velocity segments in two different ways: 1) movement-aligned, i.e., keeping the data aligned to each participant's movement onset as just described, and 2) time- aligned, i.e., using the movement onsets of only one of the two participants (subject 'A' for convention) as reference temporal markers to re-align her/his partner's data (subject 'B'; Figures 12A and 12B). Therefore, only the second type of alignment (time-aligned) preserved the real time relationship between the two partners' velocities.

Submovement-locked analysis

For the submovement-locked analysis (Figures 12C and 12D), position data were low-pass filtered (4 Hz, two-pass Butterworth, third order) before computing velocity. Preprocessing of velocity data (i.e., segmentation, change of velocity sign, subtraction of the across-segments average) was identical to that described for the cross-correlation analysis. For one of the two participants (again subject 'A' for convention), we identified the submovements as local peaks in the velocity, i.e., data points with values larger than neighbouring values (in each velocity segment). We then segmented the same participant ('A') as well as her/his partner ('B') velocities based on the identified submovements (from - 0.6 to 0.6 s), providing with 'submovement-triggered' averages (Figure 12C). Finally, the submovement-aligned data were also used to estimate the probability of producing a submovement given a submovement produced by one's partner. Specifically, we counted the number of sub-movements (local velocity peaks) for each time point (from - 0.6 to 0.6 s) in subject 'B' velocity segments (aligned to subject 'A' submovements) and then divided these numbers by the total amount of analysed velocity segments (Figure 12D). In a similar way as performed in the cross-correlation analysis, submovements probabilities were computed for both time-aligned and movement-aligned velocity data segments. We then averaged the computed probabilities within 36 equally spaced and non-overlapping bins between - 0.6 and +0.6 s. For the control experiment, analyses were limited from - 0.3 to 0.3 s to accommodate for the shorter movement durations (Figure S3, supplementary materials).

3.1.7.3 Statistical analysis

Comparison of movement tempo (F0)

We statistically evaluated whether movements are executed at a different pace compared to the instructed one by performing one-sample t-tests (against 0.25 Hz) for all conditions (solo, dyad-in-phase/anti-phase) on the F0 peak frequency, i.e., the frequency with maximal power in the velocity power spectrum. For the solo condition, the test was applied on individual parameter estimates (df = 59), whereas for the dyadic conditions the tests were applied on couple-wise across-subjects averages of the parameter estimates (df = 29). The difference in movement rate between the in-phase and anti-phase condition was tested by means of a paired samples t-test (df = 29).

Correlation between peak frequencies

We computed the Pearson correlation across subjects for all conditions (solo, dyad-in-

phase/anti-phase) between, on one side, the F0 peak frequencies and, on the other side, the F1 and (separately) F2 peak frequencies of the individual velocity power spectra. To identify the individual peak frequencies, we used the following criteria. For F0, we just took the frequency with maximal power. For F1 and F2, we sought for local peaks in the power spectrum within frequency ranges comprised between 0.5 and 1.25 Hz and between 1.5 and 4 Hz, respectively. Subjects for which no consistent peak was identified were excluded from the corresponding correlation analysis (F1: 10, 3, 2; F2: 6, 2, 16 excluded subjects out of 60 for solo, dyad-in-phase, dyad-anti-phase, respectively). If more than one peak was identified for a given subject, we included the peak with higher power and frequency closer to the across-subjects average peak frequency (F1: 16, 12, 24; F2: 6, 6, 4 subjects out of 60 for solo, dyad-in-phase, dyad-anti-phase, respectively).

In-phase vs. anti-phase comparison of PLV

Differences in the (between-subjects) PLV between the in-phase and anti-phase conditions were statistically evaluated by means of conventional paired samples t-tests. The tests were applied separately on the PLV averaged between 0.18 and 0.34 Hz for F0, between 0.55 and 0.99 Hz for F1 and between 1.53 and 3.24 Hz for F2 (ranges defined based on the across-couples range of variation – i.e., min-max – in the corresponding PLV peak frequencies; Figure 11B).

Data stratification on F0/F1 PLV

To rule out that the difference between the in-phase and anti-phase condition in the (between-subjects) PLV at F2 depends on corresponding condition differences at F0 and/or F1, we used a data stratification approach. We performed two separate stratifications, one aiming at levelling conditions differences in the mean PLV at F0 (i.e., between 0.18 and 0.34 Hz), and the other in the mean PLV at F1 (i.e., between 0.55 and 0.99 Hz). The distributions across-couples of the PLV at F0/F1 were compiled for the in-phase and anti-phase conditions and binned in 10 equally spaced bins. The number of couples falling in each bin for the in-phase and anti-phase condition was then equated by means of a random subsampling procedure which aims at matching as much as possible the PLV group-level condition averages (as implemented in Fieldtrip, function: ft_stratify, method: 'histogram', 'equalbinavg'). Stratification on F0- and F1-PLV led to the removal of 16 and 17 couples (out of 30), respectively. The condition difference in PLV at F2 (i.e., between 1.53 and 3.24 Hz) after stratification was then statistically evaluated by means of independent samples t-tests.

Time- vs movement-locking of submovements

We tested whether subject 'B' submovement probability depended on the (actual) time from subject 'A' submovements – and was therefore significantly different from what could be obtained if the two partners' submovements were locked to the individual movement onsets – by performing two-tailed paired samples t-tests on the probabilities computed for time- vs. movement-aligned data. The obtained p-values were then corrected for multiple comparisons across time by means of the Bonferroni method. We compared submovement probabilities before vs. after time zero by applying paired samples t-tests on the maximal probabilities computed for all subjects (subjects 'B'; n = 30) in the respective time intervals (i.e., from -0.6 to 0 s and from 0 to +0.6 s).

Single-couple analysis

Finally, we performed analyses at the couple-level. For each couple, we evaluated the symmetry of both the cross-correlation profile as well as the (subject B) submovement-locked profile by applying paired samples t-tests on the maximal values obtained before vs. after lag/time zero, respectively (Bonferroni correction was applied to correct for the multiple individual tests, n = 30).

3.1.8 Results

Rhythmicity at movement and submovement levels

By task design, movements are rhythmically organized with periodicity very close to the instructed pace. To highlight the rhythmic components of movement, we transformed the velocity time series into the frequency domain. As expected, all conditions display a major spectral peak around 0.25 Hz – referred to as F0 (Figure 10A). Moving together with a partner leads to a general speed-up as shown by the F0 frequencies being higher than the instructed movement pace for both dyadic conditions (in-phase: 0.28 ± 0.037 Hz, $p < 0.001$; anti-phase: 0.27 ± 0.037 Hz, $p = 0.002$), whereas slightly lower for solo performance (0.24 ± 0.036 Hz, $p = 0.059$; mean ± SD; one-sample *t*-tests against 0.25 Hz; Figure 10A). No difference in pace is, however, observed between in-phase and anti-phase synchronization ($p = 0.445$; paired samples *t*-test). Comparable results are obtained by calculating movement pace in a more canonical way as the inverse of the mean inter-movement interval (i.e., between successive flexions/extensions; solo: 0.24 ± 0.03 Hz, in-phase: 0.28 ± 0.02 Hz; anti-phase: 0.27 ± 0.02 Hz) as well as by examining the movement duration (solo: 2.1 ± 0.3 s, in-

phase: 1.8 ± 0.2 s; anti-phase: 1.9 ± 0.2 s). Besides the obvious F0 rhythmicity, the velocity profiles are marked by regular pulses that recur every ~300–500 ms (see Figure 9C for an example), yielding a less prominent but distinct spectral peak also in the 2–3 Hz range – indicated as F2 (Figure 10A). These pulses – otherwise called submovements – are a basic kinematic feature and are indeed present irrespective of the specific coordination mode. However, the increase in power at 2–3 Hz appears to be more sharply defined (narrow-band) for in-phase than anti-phase synchronization (see inset in Figure 10A), suggesting that submovements may be produced more regularly when subjects are engaged in the former rather than the latter type of coordination. Importantly, the F0 and F2 peak frequencies are not correlated (across-subjects), neither for solo performance (R = - 0.21, p = 0.12) nor for in-phase (R = 0.10, p = 0.43) and anti-phase (R = - 0.16, p = 0.29) coordination, indicating that submovement periodicity does not have harmonic or other (linear) relationships with the actual pace of the movements (Figure 11B, right column; note that subjects lacking clear peaks in the velocity power spectrum were excluded from the correlation analyses). The velocity power spectrum shows two additional components. One – denoted as F1 – peaks at about 0.8 Hz for dyadic coordination and slightly lower (~0.7 Hz) for solo performance, which is at about three times the mean F0 frequency in the respective conditions (Figure 10A; $p > 0.05$ for one-sample t-tests on F1 against 3*F0 in solo, in-phase and anti-phase). In sharp contrast with the submovement-related F2 component, F1 is indeed strongly and positively correlated with F0 in all conditions (solo: $R = 0.72$, $p < 0.0001$; in-phase: $R = 0.98$, $p < 0.0001$; anti-phase: $R = 0.80$, $p < 0.0001$; Figure 11B, left column) with slopes of the best-fitting lines being close to 3 for both the dyadic conditions (in-phase: 2.87; anti-phase: 2.89) but smaller for the solo condition (1.97). Because of its tight association with the rate of movement (possibly being a harmonic), F1 is of little interest in relation to movement intermittency. Finally, finger velocity shows a faster component with similar spectral properties across conditions and center frequency of ~8 Hz, which is known as physiological tremor.

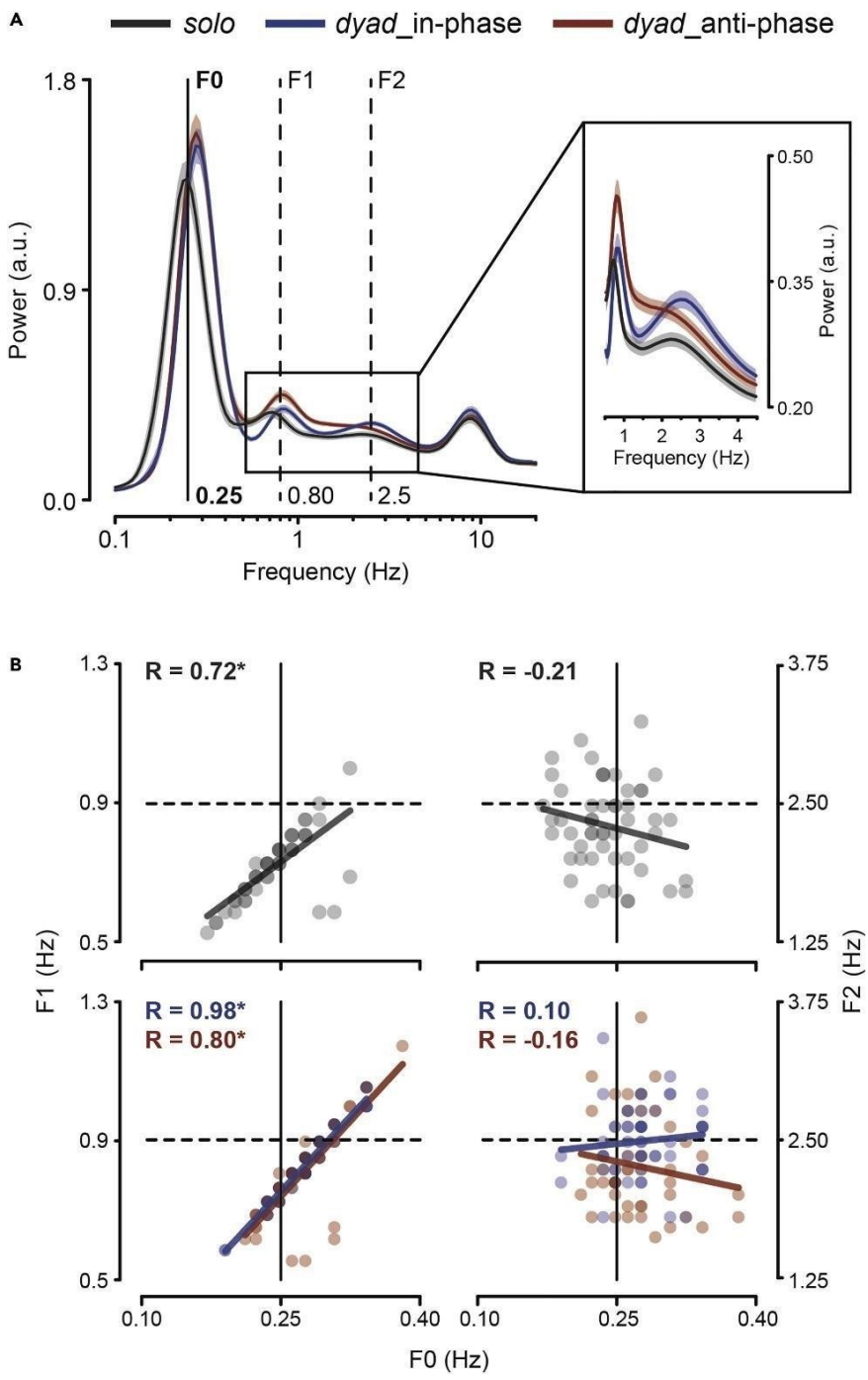

Figure 10. Rhythmicity at movement and submovement levels

A. Power spectrum of finger velocity for all conditions (solo, dyad-in-phase/anti-phase; mean ± SEM). The main spectral component peaking around the instructed movement rate (i.e., 0.25 Hz) is denoted as F0 (black solid line). The spectral components peaking around 2.5 Hz (submovement-related) and around 0.8 Hz are denoted as F2 and F1, respectively (dashed lines), and also highlighted in the inset.

B. Scatter plots showing (across-subjects) correlations of F0 peak frequencies with F1 (left) and F2 (right) peak frequencies for the solo (top) and dyadic (bottom) conditions. Data points represent individual participants. Lines represent the best-fitting linear functions (method of least squares).

Partners synchronize at both movement and submovement levels

To quantify coordination at multiple timescales during dyadic interaction, we computed the frequency- resolved phase-locking value (PLV, i.e., a measure of consistency in the phase relationship) between the two partners' finger velocities. Remarkably, interpersonal synchronization does not occur solely at F0 (and related F1) frequency as prompted by task instructions, but also at F2, which is the frequency of submovements (Figure 11A). That is, the two partners' submovements happen to be in a stable (phase) relationship. Yet, this is not true for all conditions. Indeed, submovement-level synchronization is present during in-phase coordination – as shown by the distinct F2-peak in the PLV spectrum – but nearly absent during anti-phase coordination.

We ascertained that the observed synchronization at 2–3 Hz is not artefactual or just trivial – e.g., a mere consequence of doing the same movements at the same time – by performing different control analyses. In principle, the 2–3 Hz discontinuities could be produced in a similar way on each movement, thus retaining a consistent phase across movements. Such a phase-locking of submovements to movement onset is actually very modest and comparable for the in-phase and anti-phase condition (see Figure S1, supplementary materials). Yet, because participants are moving simultaneously, submovements could appear as if they were synchronized between the two partners only by virtue of their (albeit weak) phase-locking to each partner's individual movement. If this was the case, such non-genuine submovement-level synchronization would as well be enhanced during in-phase compared with anti-phase coordination because of the greater synchrony between the two partners' movements in the former than the latter condition, which is evidenced by the correspondingly higher PLV at both F0 (p = 0.028) and F1 (p = 0.019; see bar plots in Figure 11B). Thus, to ensure that submovement-level synchronization is not a by-product of the overall better in-phase than anti-phase (movement-level) synchronization, we used two complementary analytical strategies. Both of them aim at matching the conditions (in-/anti-phase) for movement-level synchronization, but the first analysis does so at the group level whereas the second one at the couple level. We first used a data stratification approach that consists of subsampling the couples (by means of a random iterative procedure) so that the mean PLV at F0 and (in separate runs) F1 is equated as much as possible between the two conditions. As shown in

Figure 11B, both types of data stratifications (i.e., on F0 and F1) leave the pattern of results virtually unchanged, with synchronization at the submovement frequency (F2) being significantly stronger during in-phase than anti-phase coordination ($p < 0.001$; independent samples *t*-tests). As for the second analysis, we computed again the between-subjects PLV, this time not on the entire velocity time series (shown in Figure 11A) but on shorter 2-s segments (covering approximately the duration of one single movement) that are time-aligned to the onset of each partner's individual movement. In this way, we artificially compensated for the temporal asynchronies between the two partners' movements, leveling the discrepancy in synchronization performance between the two conditions. Remarkably, this alignment on-movement procedure severely disrupts synchronization at 2–3 Hz for the in-phase condition, making it as weak as that observed for the anti-phase condition ($p = 0.215$; paired-samples *t*-test; see Figure S1, supplementary materials). Altogether, these results decisively exclude that the observed phenomenon is explained by any systematic locking of submovements to movement dynamics and/or the better in-phase vs anti-phase movement synchronization performance; rather, they suggest a true and real-time coadaptation of submovements between the two partners.

Interpersonal synchronization at submovement frequency is also confirmed in two additional experimental conditions. In the first one, we change the hand posture and movement axis (from horizontal to vertical) and show that the effect is independent from the congruency between the two partners' flexion/extension movements during in-phase and anti-phase coordination (see Figure S2A, supplementary materials). In the second one, we show that a similar phenomenon persists when the task involves whole-arm movements (on the horizontal and vertical plane), thereby extending our observations to multi-joint action coordination (see Figure S2B, supplementary materials).

Thus, submovement-level synchronization seems to be largely independent from the effector as well as the congruency between the partners' movements, but highly dependent on their (visuo-)spatial alignment. In fact, the main difference between the two coordination modes is the spatial alignment of the effectors' end-points (i.e., the fingertips): a 0° and 180° difference in position is required for in-phase and anti-phase coordination, respectively. Consistently with task requirements, the (across-couples) distribution of the mean phase lag at F0 between the two partners' kinematics is strongly concentrated around 0-deg for in-phase and 180-deg for anti-phase coordination (Figure 10A, polar plot on top). The same phase relationship as for F0 is also observed for the related F1, although with a less degree of consistency. Surprisingly, synchronization at the submovement level (Figure 10A, polar

plot on bottom) is characterized by an opposite, ~180° relative phase shift with respect to what is established at the movement level (F0) during in-phase coordination (phase lags are relatively scattered during anti-phase coordination, in agreement with the PLV lacking a distinct F2 peak in this condition). In other words, submovements during in-phase synchronization are inter- locked in the two partners and seem to follow one another with an alternating, counterphase pattern.

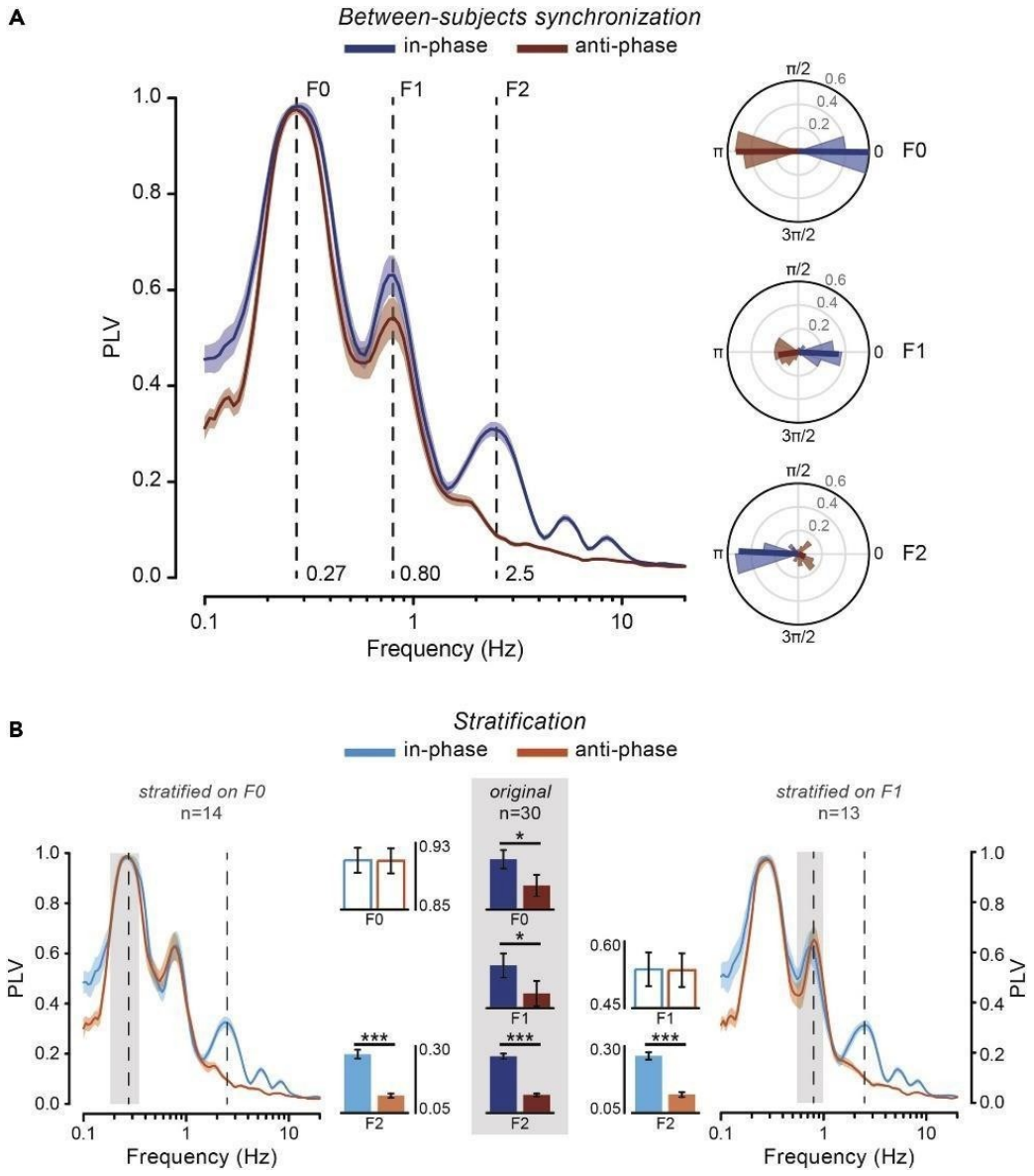

Figure 11. Partners synchronize at both movement and submovement level

A. Between-subjects PLV spectrum for the in-phase and anti-phase condition (left; mean ± SEM). Polar plots (right) showing the across-couples distribution of the mean phase difference (phase lag) for F0 (top), F1 (middle), and F2 (bottom).

B. PLV spectra after data stratification (at the group level) on F0 (left) and F1 (right). Bar plots show mean PLV in the relevant frequency ranges for the original (middle; n = 30) and stratified (left, n = 14; right, n = 13) data. Error bars indicate ± SEM. *p < 0.05, ***p < 0.001. See also Figures S1 and S2, supplementary materials.

Bidirectional modulation of submovements

To further clarify the nature of submovement-level synchronization, we computed the cross-correlation between the two partners' (unfiltered) velocities. We first selected data segments that correspond approximately to single movements, i.e., from movement onset to mean movement duration. To discard the main contribution deriving from slow and movement-locked components, we subtracted from each segment the mean velocity profile over all segments. We then computed the (between-subjects) cross-correlation either by keeping both partners' data aligned to the individual movement onset (as just described) and thus misaligned in time (movement-alignment), or by (re)aligning one of the two partners' data to the other partner's movement onset (subject ''A'' by convention) and thus restoring their real alignment (time-alignment). The cross-correlation profile shows a striking difference between the two types of alignments, which is far most apparent for the in-phase condition (Figure 12A). Correlation for the movement-aligned data is maximal at lag zero and slowly declines for lags up to ± 0.6 s, reflecting residual (not accounted for by the average subtraction) covariation in movement dynamics between the two partners. Conversely, correlation for the time-aligned data is relatively low at lag zero but sharply increases at symmetrical lags of about ± 0.18 s. This curious double-peaked correlation profile most certainly reflects the succession in the partners' submovements. Indeed, the two cross-correlation peaks are separated by a (lag) interval of almost 0.4 s, closely matching the oscillatory period of submovement production (i.e., 2.5 Hz). Whereas the two peaks are evident in the in-phase condition, two flattened humps are barely detectable at longer lags of about ± 0.25 s in the anti-phase condition (Figure 12A, right), reflecting the fact that generation and interpersonal locking of submovements occurs rather erratically and at a slightly lower frequency in this coordination mode. The rhythmic 2.5-Hz co-variation between the two partners' kinematics during in-phase coordination and its impairment during anti-phase coordination is further emphasized by taking the difference between the two cross-correlations (time- vs movement-aligned) that yields, for the first condition, an oscillating profile, whereas for the second, an almost flat profile.

If the two partners' submovements do alternate with regularity (in-phase condition), by locking the velocity of one participant to his/her own partner's submovements, the probability of observing a submovement in the former should not be uniform over time but relatively high/low at specific times (corresponding to the lags of high/low cross-correlation and to half period of the submovement frequency). Figures 12C and 12D show that this is exactly what we observe. We identified submovements as velocity peaks occurring within the movements performed by only one of the two participants in the couple (again subject ''A'' by convention) and then segmented both participants' velocities based on the identified peaks (from - 0.6 to +0.6 s). The submovement-locked velocity for subject ''A'' shows the expected peak at time zero and two smaller peaks at about ± 0.35 s, reflecting 2–3 Hz periodicity in submovements generation. Most interestingly, subject ''B'' velocity (locked to subject ''A''submovements) also shows an oscillating pattern, which is apparent for the in-phase and less so for the anti-phase condition (Figure 12C). The probability of observing a submovement (i.e., a velocity peak) in subject ''B'' is clearly modulated as a function of time relative to his/her partner's submovements generation (time-aligned data) and is significantly different (higher/lower) than that obtained for movement-aligned data at multiple and regularly interspersed time points, closely matching the submovements rate (Figure 12D). Analogously to what was reported for the cross-correlation profiles, subject ''B'' submovements probability is maximal at relatively shorter (± 0.18 s) and longer (± 0.3 s) times for in-phase and anti-phase, respectively, suggesting faster (besides tighter) between-subjects alternation of submovements in the former than the latter condition.

We further asked a different sample of couples to coordinate in-phase at multiple movement paces (0.25, 0.5, 0.75, and 1 Hz; Figure S3, supplementary materials). The two partners systematically alternate their submovements at 0.25 Hz (replicating the main results) as well as when moving at double this speed, i.e., at 0.5 Hz. Though qualitatively very similar, submovements coordination is however noisier at higher paces (Figure S3D, supplementary materials). Notably, in line with the known speed-up effect during interpersonal motor coordination, partners were always keeping a faster pace than instructed (mean movement duration ± SD: 1.83 ± 0.12 s [$p = 0.0016$; t-test against 2 s], 0.89 ± 0.15 s [$p = 0.046$; t-test against 1 s], 0.54 ± 0.09 s [$p = 0.0039$; t-test against 0.66 s], and 0.4 ± 0.04 s [$p = 0.0068$; t-test against 0.5 s] for the 0.25-, 0.5-, 0.75-, and 1-Hz pace, respectively). As a consequence, at 0.75 and 1 Hz, actual movement duration de facto approaches the average interval (period) between successive submovements (~0.4 s), drastically reducing the probability of producing at least one submovement in each single movement. In other terms, movements

were most often executed in a one-shot, ballistic way and this could only (and trivially) have detrimental effect on the phenomenon under investigation here.

To ascertain that submovements are truly co-modulated in a bidirectional way during the real online interaction, we examined the results also at the single couple level. In fact, the observed (group-level) symmetry might conceal asymmetrical results in individual couples (e.g., subject A's submovements influencing to a larger extent subject B' submovements than vice versa) that are mixed up in the average owing to the arbitrary assignment of subject A/B. Yet, significant asymmetry in the cross-correlation and in the submovement-locked profiles is only found in 3 couples out of 30 (paired samples t-tests on maximal correlation/velocity before vs after lag/ time zero), indicating that a bidirectional co-regulation of submovements is indeed occurring in the great majority of the couples.

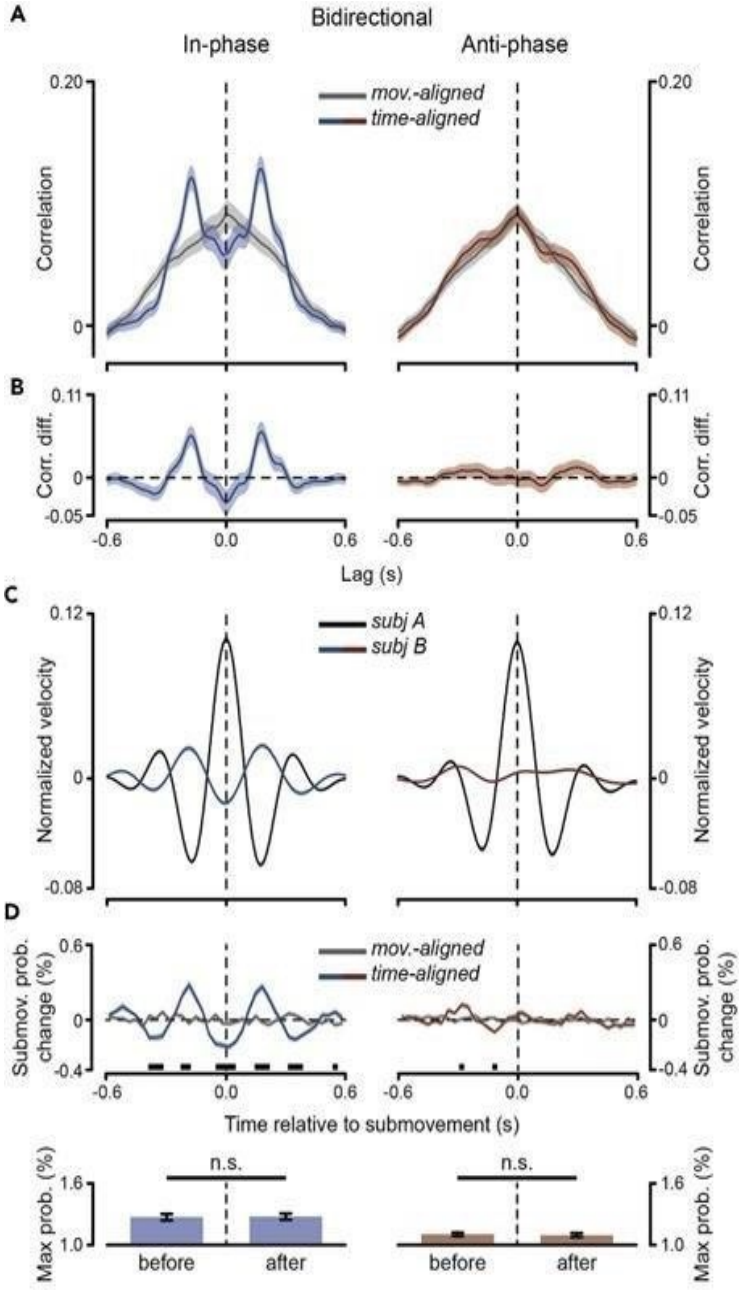

Figure 12. Bidirectional modulation of submovements

A. Cross-correlation between the two partners' (unfiltered) velocities during in-phase (left) and anti-phase (right) synchronization in the ''Real partner'' task (bidirectional interaction). The cross-correlation is computed between velocity data segments (~2 s) that are either movement-aligned, i.e., aligned to each partner's movement onset, or time-aligned, i.e., aligned to one of the two partners (subject ''A'' by convention) movement onset, thus preserving their real time alignment (mean ± SEM).
B. Difference between the time- and movement-aligned cross-correlation profiles (mean ± SEM).
C. Velocity for both partners – subjects ''A'' and ''B'' – locked to submovements generated by one partner in the couple – i.e., subject ''A'' by convention (''Real partner'' task; mean ± SEM).
D. Submovement probability (expressed as deviation from mean probability) for one participant (subject ''B'') as a function of the actual time (time-aligned) or of time relative to movement onset (movement-aligned) from submovements generated by his/her partner (subject ''A''; top panels). The black horizontal bars indicate the time points that survive two-tailed t-test statistics on movement- vs time-aligned data (Bonferroni-corrected for multiple comparisons across time). Maximal submovement probabilities (for subject ''B'' time-aligned to subject ''A'') computed separately before and after time zero (i.e., before and after subject ''A'' submovements; bottom panels).

3.1.9 Supplementary materials

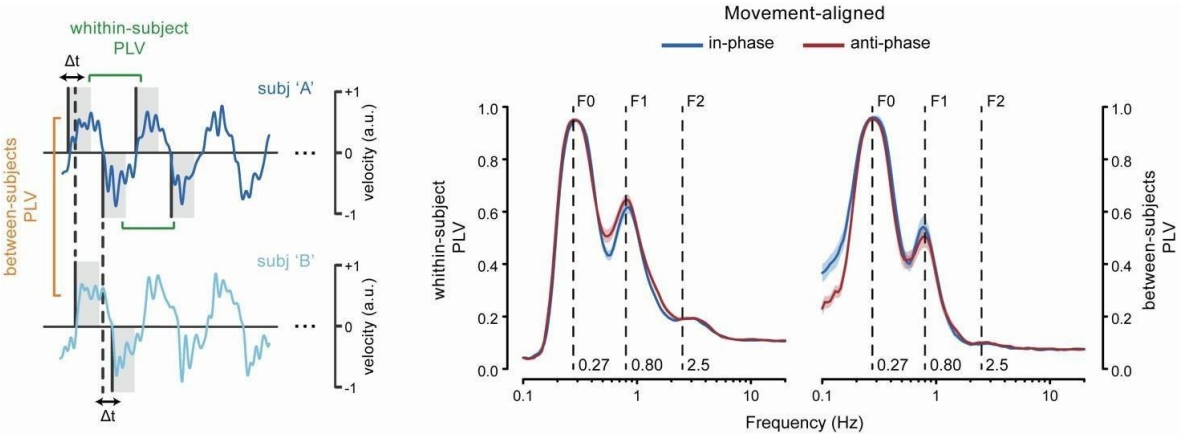

Figure S1. Movement-locked control analyses: submovement-level interpersonal synchronization is not explained by phase-locking of submovements to movement onset, related to Figure 3. The left panel shows example traces of two partners' finger velocity during in-phase synchronization ('Real partner') and a schematic of the data segmentation and analyses. Data are segmented in 2-s segments (corresponding to the instructed movement duration) locked to the onset of single movements performed by each partner. The phase-locking value (PLV) is computed either within-subject (n = 60) – i.e., across the movements performed by the same participant (separately for flexions and extensions and then averaged across movement types) – or between- subjects (n = 30) – i.e., between the two partners' movements. The right panels show the within-subject and between-subjects PLV spectra for both the in-phase and anti-phase conditions (mean ± SEM).

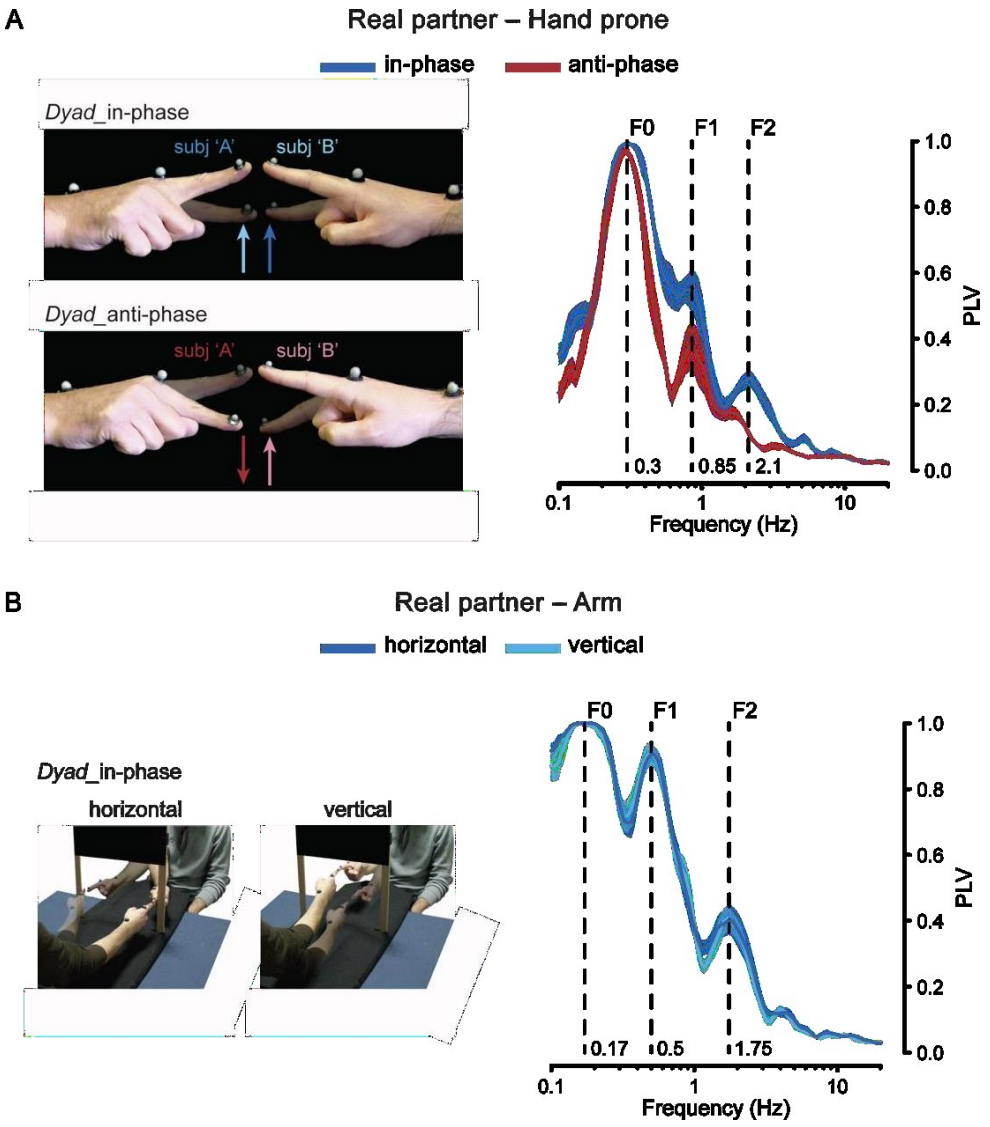

Figure S2. Secondary tasks: submovement-level interpersonal synchronization does not depend on movement congruency and generalizes to multi-joint actions, related to Figure 3. (A) left. Illustration of the 'Real partner – Hand prone' secondary task. Participants keep their right hand in a prone posture and move the index finger along the vertical axis. As opposed to the primary task (main Figure 1A, B), the two partners perform simultaneously the same type of movement (either flexion or extension) to attain in-phase coordination (i.e., move towards the same direction), whereas they perform different types of movements (as one performs flexion, the other performs extension and vice versa) to attain anti-phase coordination (i.e., move towards opposite directions). right. between- subjects PLV spectra for the in-phase and anti-phase condition (n = 10; mean ± SEM). (B) left. Illustration of the 'Real partner – Arm' secondary task. Participants perform whole-arm movements (primarily around the elbow joint) along either the horizontal or vertical inner dimensions of the window (~40x40 cm) delimited by an interposed panel. The task involves tracking of each other's movement to keep the respective fingertips spatially aligned (dyad-in-phase only). Given the larger movement amplitude compared to the primary task, the instructed movement rate is reduced to 10 bpm (i.e., ~0.17 Hz). right. between-subjects PLV spectra for the horizontal and vertical condition (n = 10; mean ± SEM).

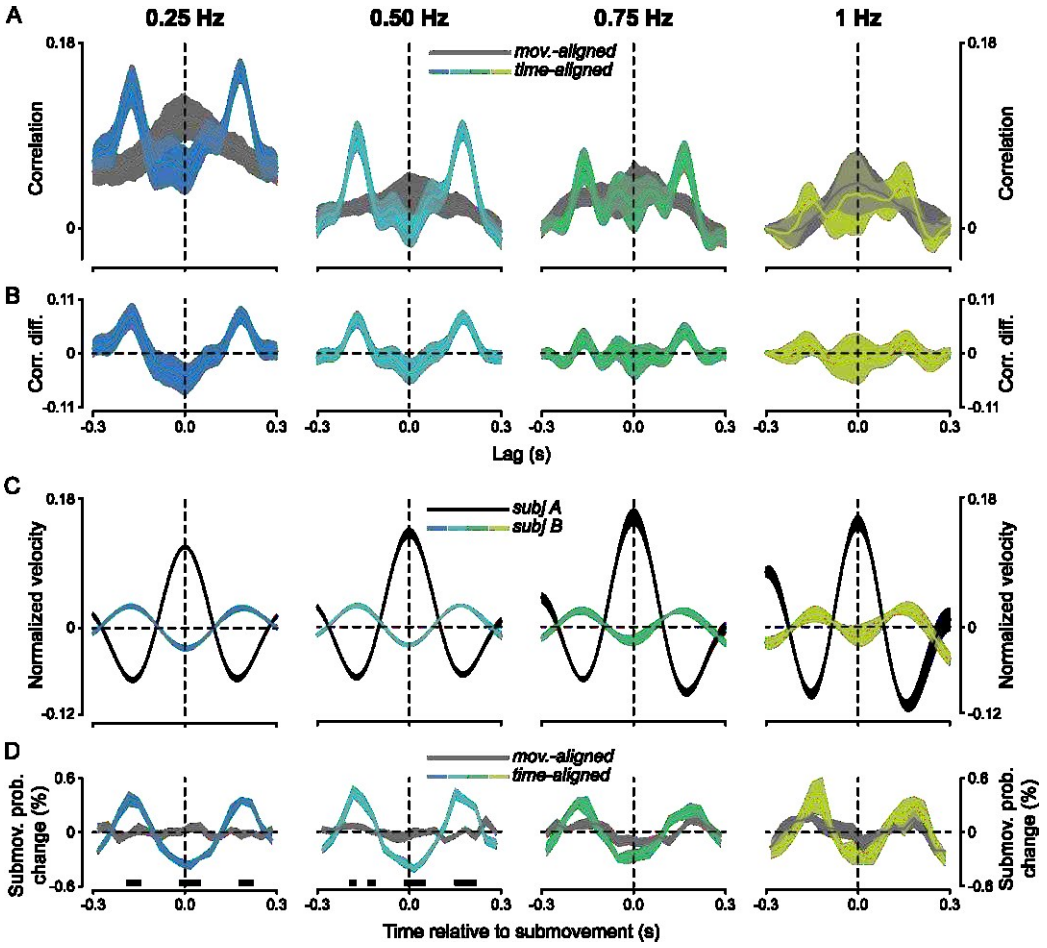

Figure S3. Control experiment: speed-dependency of submovement-level interpersonal synchronization, related to Figure 4. (A) Cross-correlation (same as in Figure 4A,B but for a restricted lag range to accommodate the shorter movement durations) computed between the finger velocities of two partners performing the 'Real partner' task at multiple movement paces (i.e., 0.25, 0.5, 0.75 Hz [n=10] and 1 Hz [n=5]). The cross-correlation is computed between velocity data segments (of length equal to average movement duration) that are either movement-aligned, i.e., aligned to each partner's movement onset, or time-aligned, i.e., aligned to one of the two partners (subject 'A' by convention) movement onset, thus preserving their real time alignment (mean ± SEM; see Methods). (B) Difference between the time- and movement-aligned cross-correlation profiles (mean ± SEM). (C) Velocity for both partners – subjects 'A' and 'B' – locked to submovements generated by one partner in the couple – i.e., subject 'A' by convention (same as in Figure 4E; mean ± SEM). (D) Submovement probability (expressed as deviation from mean probability) for subject 'B' as a function of the actual time (time- aligned) or of time relative to movement onset (movement-aligned) from submovements generated by subject 'A' (same as shown in Figure 4F). The black horizontal bars indicate the time points that survive two-tailed t-test statistics on movement- vs. time-aligned data (Bonferroni-corrected for multiple comparisons across time).

Chapter 4

4.1 Study 3. *Inter-personal motor coordination goal: Bimanual Task*

4.1.1 Abstract

In this study, we aimed to combine the aspects of interpersonal and bimanual coordination, which we have previously investigated separately, by asking participants to use both hands to coordinate with each other. Time-domain analysis was performed on the kinematic data of the index fingers of both interacting participants, which were recorded by a motion-capture system. Our analysis revealed an alternating pattern of submovements emission between the interacting partners' index finger during the in-phase condition, suggesting mutual regulation between them. However, no relationship was observed during the anti-phase condition. When we analysed the timing of submovements emission within a single participant's hands while interacting with a partner, we found that submovements were emitted almost simultaneously in both the in-phase and anti-phase conditions, as if they were emitted by a single controller.

4.1.2 Personal contribution

I performed the experiment together with my colleague Dr. Marco Emanuele, recorded the data with my colleague Dr. Chiara Esposto and performed all the analyses using codes I wrote in Matlab under the supervision of Dr. Alice Tomassini and Prof. Alessandro D'Ausilio. In the near future we plan to write a paper about the data herein presented.

4.1.3 Sample

Twenty participants (10 females and 10 males) were recruited for this study to form ten gender-matched couples (age: 23.4±3.05 years, mean±SD). All participants had normal or

corrected to normal vision and they self-reported being right-handed. This was also verified by the experimenters who checked the handedness of the participants while they filled out ethics forms before the experiment.

4.1.4 Procedure

Participants forming a gender-matched couple were asked to sit at a table in front of each other (~1 m apart) at the opposite sides of a panel, which prevented them from seeing their faces (Figure 13A). They were asked to keep the ulnar sides of their left and right forearms resting on the table and hold their hands in a closed fist posture, with only their own left and right index fingers pointing towards their partner's corresponding index fingers (Subject A's right/left index fingers and Subject B's left/right index fingers distance: ~ 1 cm; Subject A's and B's left-right index fingers distance: ~ 8 cm). This way, movements of Subject A's right and left index fingers corresponded to movements of Subject B's left and right index fingers, respectively. Participants were then asked to perform rhythmic flexion-extension movements of their index fingers around the metacarpophalangeal joint as synchronously as possible during each trial. They were asked to move their index fingers in-phase (i.e., movement in the same direction) or anti-phase (i.e., movement in the opposite direction) at a reference pace of 15 bpm (flexion-extension movement duration: 4 sec; flexion/extension movement duration: 2 sec) depending on the condition (Figure 13B). Participants familiarized themselves with the requested pace before the experiment by listening to a metronome, which was silenced during the trials and briefly replayed at the start of each condition. In the In-phase Condition, Subjects A and B were instructed to perform the first movement towards the right and left, respectively, whereas in the Anti-phase Condition, they were asked to perform the first movement both towards the right (refer to Figure 13B). Participants performed two blocks, one for the In-phase Condition and one for the Anti-phase Condition, each composed of two 2.5 minute-long trials interspersed by a brief break. The total duration of the experiment was 12 minutes. The condition order was randomized across couples. The data were analysed on both between-subjects pairs of Subjects A' right/Subjects B' left and Subjects A' left/Subjects B' right index fingers (Figure 15A, Interpersonal analysis) and within-subjects own right and left index fingers, i.e., between Subjects A' right and left index fingers and Subjects B' right and left index fingers (Figure 15B, Intrapersonal analysis).

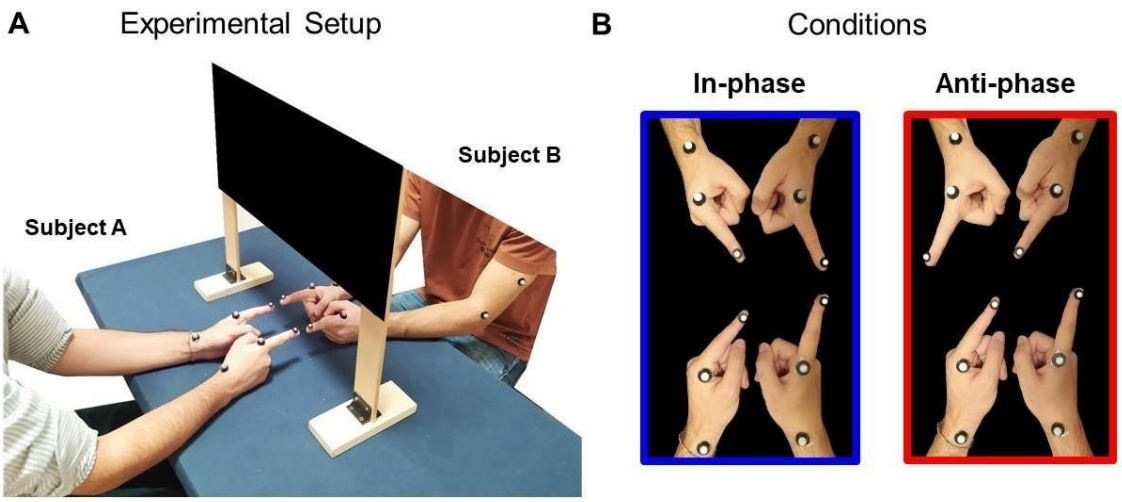

Figure 13. Experimental Setup and Procedure

A. Pairs of participants were seated at a table facing each other, with a panel positioned in between to prevent them from seeing each other's faces. They were instructed to rest the ulnar sides of their left and right forearms on the table and clench their hands into fists, pointing only their left and right index fingers towards their partner's corresponding index fingers.
B. We asked participants to perform rhythmic flexion-extension movements at a 15 bpm pace, as synchronously as possible, either in-phase or anti-phase., with both their index fingers.

4.1.5 Kinematic data recording

We recorded the kinematics of movements using a ten-camera motion capture system (Vicon Nexus, with a sampling rate of 300 Hz) along three axes: mediolateral (X), anteroposterior (Y), and vertical (Z). However, we limited our analysis to the main mediolateral movement axis (X-axis). To collect position data, we placed retro-reflective markers on the distal phalanxes of the right and left index fingers (marker diameter: 6.4 mm). Figure 13A shows two additional markers placed on the metacarpophalangeal joint (marker diameter: 9.5 mm) and the styloid process of the radius (marker diameter: 9.5 mm) of both hands for reconstruction purposes. Furthermore, we placed one more retro-reflective marker on Subjects A' left lateral epicondyle of the humerus (LEH), two more on Subject B's right LEH and shoulder, and three more on Subjects B' left LEH, middle triceps, and shoulder (not all markers are visible in Figure 13A) to distinguish the different hands within and between subjects.

4.1.6 Time Domain Analysis

Analyses were performed with custom-made codes programmed in MATLAB computing environment. Data were filtered using FieldTrip Toolbox.

Segmentation and pre-processing of velocity data

The onset of each flexion/extension movement was identified on low-pass filtered (3 Hz, two-pass Butterworth, third order) position data. The movement onsets were defined as peaks in position data that corresponded to the inversion of movement direction: from flexion to extension and vice versa. Peaks were detected on position data whose sign was adjusted to be positive in all recorded trials. Thus, we circumvented the negative signs of extension movements with respect to the main axis of the movement. The identified movement onsets were then visually checked on both position data and on corresponding velocity data. In the latter case, we ascertained that the peaks detected in position data coincided with the samples where the velocity passed through zero. All errors in data segmentation were manually corrected: Segments in which participants lost the coordination mode with their interacting partner's index fingers were removed from the analysis. Likewise, all segments with durations greater than or less than 2.5 standard deviations from the mean movement duration (computed trial-wise on all retained segments of single participants' index fingers) were excluded from further analysis.

Finally, the time stamps of the movement onset were used to segment the velocity data, which was computed as the first derivative of the position data low-pass filtered at 4 Hz (two-pass Butterworth filter, third order). All the analysis were performed on velocity data pre-processed as follow:

1. The sign of the velocity segments was changed to ensure that all velocity segments were positive (first step: change of velocity sign).
2. The velocity was normalized based on the maximal speed calculated trial-wise for each index finger (second step: velocity normalization).
3. The average velocity profile was subtracted from each index finger to remove movement-related components (third step: average velocity profile subtraction).

Temporal characterization of movements at macroscopic and microscopic scales

To analyse the temporal synchronization at the macroscopic level of the movement (Movement Synchronization; Figure 14A), we first calculated the mean and standard deviation of the absolute differences in movement onsets between participants' index fingers. Specifically, we calculated such absolute differences between the movement onsets of Subjects A' right-Subjects B' left index fingers and Subjects A' left-Subjects B' right index fingers. Next, we calculated the grand average of these means and standard deviations across all couples for each condition.

At the microscopic level, we evaluated the mean and variability of submovement emission to measure the timing between submovements (Inter-submovements Time; Figure 14B). To this end, we identified submovements as local peaks in the velocity segments of each individual participant's right and left index fingers. We then calculated the mean and standard deviation of the differences in submovements onset (trial-wise), taking into account both index fingers of each participant. Finally, we calculated the grand average of the means and standard deviations of inter-submovements onsets across all participants, for each condition.

Submovement-locked analysis (qualitative analysis) and Submovement-locked probabilities (quantitative analysis)

For the submovement-locked analysis (qualitative analysis, see Figures 15A and 15B upper panels), we detected the submovements as local peaks in velocity segments of participants' right index fingers. We then segmented the velocity segments of the right and corresponding left index finger within a time window of ±0.6 seconds, centred around the identified submovements in the right hand. More specifically, to characterize the temporal relationship between submovements emitted by both hands of interacting participants, we identified the submovements of both Subjects A and B' right index fingers to segment the corresponding Subjects B and A' left index fingers (Interpersonal analysis). While, to analyse the temporal relationship linking submovements emitted by single participants' both hands – during the interpersonal motor coordination task – we segmented the single participants' left index fingers on the basis of the identified submovements in their own right index fingers (Intrapersonal analysis). Importantly, the velocity segments of the left index finger were preliminarily time-aligned with the movement onsets of the right index finger to restore the

actual temporal relationship between between the movements of both hands as they occurred during the experiment. The velocity segments of the left index finger were also used to calculate the probabilities of submovements emission, based on either the submovements of interacting participant' right hand (Interpersonal analysis) or the submovements of the participant's own right hand (Intrapersonal analysis) (quantitative analysis, Figures 15A and 15B lower panels). This probability was estimated by counting the number of submovements identified as local peaks in the velocity segments of the left index finger for each time point, ranging from -0.6sec to +0.6 sec relative to the submovements detected in the right index finger. The sum of submovements detected in each time point was then divided by the total number of velocity segments based on the identified submovements in the right index finger. Finally, the left hand probability of emitting a submovement at each time point was expressed as a percentage deviation from the mean probability of submovement emission computed across the entire segment duration, by summing the probability associated with each time point. The computed probabilities were then averaged within 36 non-overlapping equally spaced bins, in each trial. For statistical comparison purposes, we also derived probabilities from surrogate data. The shuffling procedure was implemented through an iterative (5000 iterations) random assignment of velocity segments of the left index finger to velocity segments of the right index finger, in order to destroy the actual sequencing of movements as they were emitted during the trial. The estimation of the probability and the definition of binned probabilities for surrogate data were identical to the procedure described for the quantification of the probabilities of the original data.

4.1.7 Statistical Analysis

Comparison of movements at macroscopic (Movement Synchronization) and microscopic (Inter-submovements Time) scales

We used a paired sample t-test to test whether the means and the standard deviations of the absolute differences in movement onsets (Subjects A and B' right hands minus corresponding Subjects B and A' left hands), were statistically different across 10 couples for in-phase and anti-phase coordination mode (Movement Synchronization, Figure 14A). Likewise, we used a paired samples t-test to test whether there were any significant

difference of the means and of the standard deviations of the inter-submovement onsets computed across the 20 participants' both hands (Inter-submovements Time, Figure 14B).

Original binned time-locked probabilities vs. surrogate binned probabilities

We performed a two-tailed t-test that was Bonferroni-corrected for the number of bins considered ($p < 0.0014$) to assess whether there were statistically significant differences in mean probabilities computed between-subjects (Interpersonal analysis) or within single-participants (Intrapersonal analysis) on original vs. surrogate data.

4.1.8 Results

Participants were able to synchronize their right index finger movements with their interacting partner's corresponding left index finger movements significantly better ($t_9 = -3.321$, $p = 0.009$) during in-phase (M: 142.178 ms; SE: ± 9.269 ms) than anti-phase (M: 174.471 ms; SE: ± 7.557 ms) conditions. However, no significant difference ($t_9 = -2.177$, $p = 0.057$) was found in the variability of movement emission between in-phase (M: 107.789 ms; SE: ±7.721 ms) and anti-phase (M: 129.890 ms; SE: ± 6.147 ms) conditions. At the Inter-submovements Time Level, participants emitted submovements significantly more frequently ($t_{19} = -2.778$, $p = 0.012$) and consistently ($t_{19} = -3.895$, $p < 0.001$) during in-phase than anti-phase conditions, as indicated by the means (In-phase M: 345.757 ms; SE ± 4.109; Anti-phase M: 353.949 ms SE: ± 3.896 ms) and standard deviations (In-phase M: 123.782 ms; SE ± 2.44; Anti-phase M: 132.572 ms SE: ± 2.11 ms) of the difference in submovements emission.

In summary, the results suggest that interacting partners were better able to synchronize their movements and produce submovements more rapidly and consistently during in-phase than anti-phase coordination modes.

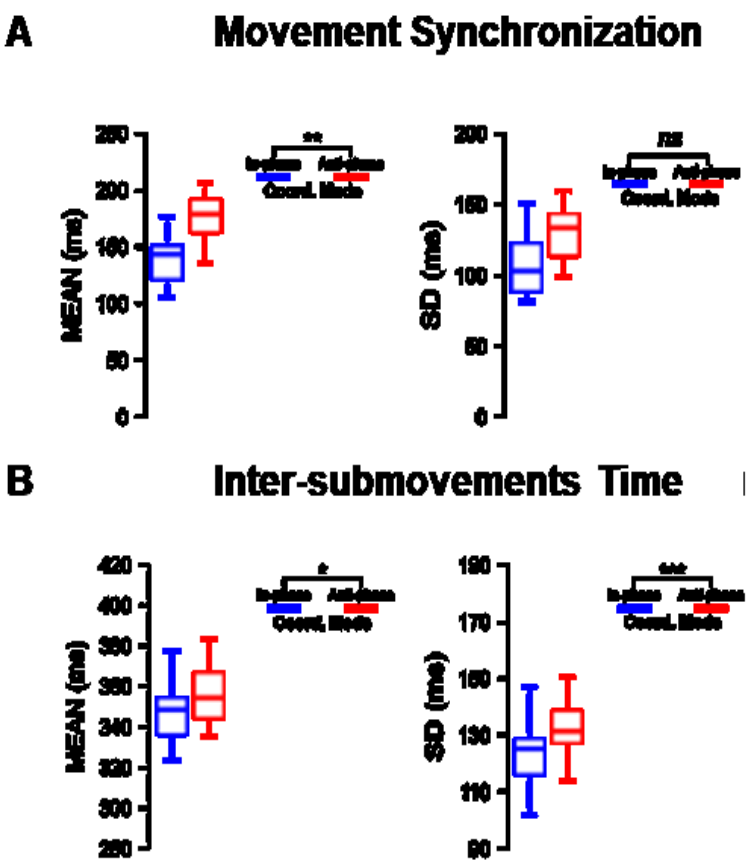

Figure 14 Temporal characterization of movements at macroscopic and microscopic scales

A. Mean and standard deviation of the absolute differences in movement onsets between participants' index fingers computed across couples for each condition.

B. Mean and standard deviation of the differences in submovements onset, detected as local peaks in the velocity segments of single participant's right and left index fingers, computed across subjects for each condition.

When analysing the temporal relationship between the submovements produced by the hands of two interacting participants, we found a pattern of results similar to that of the previous study (Study 2). Specifically, we observed that during in-phase coordination mode, the submovements produced by one participant alternated over time with respect to the submovements produced by the interacting partner. This did not happen when participants were required to coordinate with an anti-phase coordination mode. As seen in Figure 15A (Interpersonal, upper panel on the left), the submovements emitted by Subjects A/B' left index fingers slightly anticipate and follow the ones emitted by the corresponding Subjects B/A' right index fingers, giving rise to a characteristic double peak profile during the In-phase Condition. Conversely, the almost flat profile observed during the Anti-phase Condition seems to indicate no relation between the submovements emitted by Subjects A/B'right and Subjects B/A' corresponding left index fingers (Figure 15 A, upper panel on the right). Notably, when the relationship between a single participant's own hands was

analysed, the submovements of the left index finger seemed to be emitted almost simultaneously with those produced by the right index finger, regardless of the in-phase or anti-phase coordination mode. Indeed, the submovements of the left index fingers showed a profile witha clear peak occurring at the same time as the submovements produced by the right index fingers, during both In-phase and Anti-phase Conditions. This pattern of results is exactly the same as what we found in the first study (Study 1), where participants were required to coordinate either in-phase or anti-phase movements of their index fingers with their eyes closed. The similarity of the results could be explained by the fact that in this study, even though the participants had visual feedback, they were required to pursue a goal of interpersonal coordination and were therefore somehow "blind" to the attempt to coordinate the movements of their own indices.

The qualitative patterns of modulation, observed by time-locking the submovements of the left index fingers with the submovements detected in the velocity segments of the right index fingers, were confirmed by a one-tailed t-test Bonferroni corrected for multiple comparisons. The analysis was based on the original versus surrogate binned probabilities (Figures 15A and 15B lower panels) of left index finger submovement emission, given the submovement produced by the right index finger. Specifically, the analysis conducted between the hands of the two interacting participants revealed that the binned probabilities of emitting submovements in an alternating trend during the original vs. surrogate in-phase coordination mode were significantly different at two temporal moments, preceding and following the emission time of submovement in the right index finger. Conversely, no significant differences were observed between original vs. surrogate during anti-phase coordination mode. When considering the relationship between hands within participants (Intrapersonal analysis), the binned probabilities computed on original vs. surrogate data of the left index fingers were statistically significant in a temporal range synchronous with the submovements produced by the right index finger for both in-phase and anti-phase coordination modes (Intrapersonal, Figure 15B).

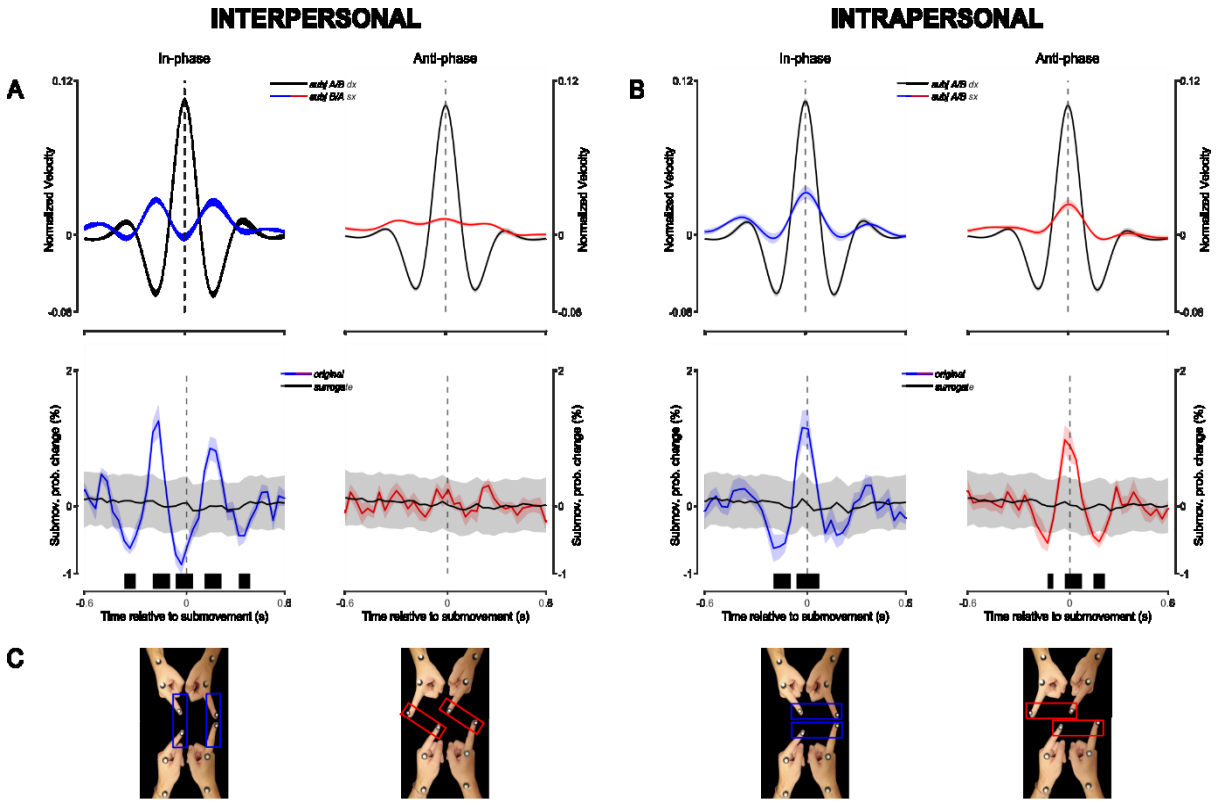

Figure 15. Interpersonal and Intrapersonal modulation of submovements.

Upper Panel A. Velocity of participants' left and right index fingers time-locked to submovements generated by theinteracting partner's right index finger (mean ± SEM).

Lower Panel A. Submovement probability (expressed as deviation from mean probability) for participants' left finger indexes as a function of the actual time (original time-aligned data) or of random assigned velocity segments (surrogate data) from submovements generated by interacting partner's right index finger. The black bars indicate the time points that survive two-tailed t-test statistics on time-aligned original data vs. surrogatedata (Bonferroni-corrected for multiple comparisons across time).

Upper Panel B. Velocity of single participants'left and right index fingers locked to submovements generated by their own right index finger (mean ± SEM).

Lower Panel B. Submovement probability (expressed as deviation from mean probability) for participants' left finger indexes as a function of the actual time (original time-aligned data) or of random assigned velocity segments (surrogate data) from submovements generated by their own right index fingers. The black bars indicate the time points that survive two-tailed t-test statistics on time-aligned original data vs. surrogate data (Bonferroni-corrected for multiple comparisons across time).

C. The colored boxes drawn on the hands pictures highlight the relevant relationship that is being considered for the analysis of submovement coordination, i.e., whether the relationship between the submovements produced by the hands of the two interacting partners (interpersonal) or by the two hands of the same participant (intrapersonal) is being analyzed.

Chapter 5

5.1 Study 4. *Virtual motor coordination goal: Unimanual Task (Healthy subjects)*

5.1.1 Abstract

In this study, we aimed to test the validity of the results concerning the mutual adaptation of submovements in two interacting partners during an interpersonal coordination task by replacing one member of the pair with a virtual partner. The virtual partner was represented by a dot that moved on a computer screen according to a pre-recorded human kinematics and was unresponsive to the real partner's movements. Time-domain analysis revealed that submovements emitted by real participants systematically follow the submovements emitted by the moving dot suggesting a unidirectional modulation of the moving dot's submovements on real participants' submovements.

5.1.2 Personal contribution

The text and figures presented below are retrieved from the already published paper *Tomassini, A., Laroche, J., Emanuele, M., Nazzaro, G., Petrone, N., Fadiga, L., &D'Ausilio, A. (2022). Interpersonal synchronization of movement intermittency. Iscience, 25(4), 104096* (https://doi.org/10.1016/j.isci.2022.104096) in which I was involved in data collection, and are presented separately as they serveas the foundation for the study 5.

5.1.3 Sample

Twenty participants (10 females) (age 23.9 ± 4 years, mean ± SD) took part to the experiment. All participants were right-handed (by self-report) and had normal or corrected-to-normal vision. The study and experimental procedures were approved by the local ethics

committee. Participants provided written, informed consent after explanation of the task and experimental procedures, in accordance with the guidelines of the local ethics committee and the Declaration of Helsinki.

5.1.4 Procedure

Participants were seated at a table in front of a computer screen, with the ulnar side of their right forearm resting on a rigid support. They were asked to perform flexion-extension movements of their index finger about the metacarpophalangeal joint, while tracking a visual dot (size: 1.5 cm, position: 7 cm above the bottom screen edge) that moved horizontally on the computer screen in front of them (Figure 16). The dot velocity corresponded to the velocity of the index fingertip recorded on author A.T. while she was taking part in the solo performance of the primary task described in Study 2. Depending on the condition, participants were asked to track the dot kinematics either in-phase or anti-phase.

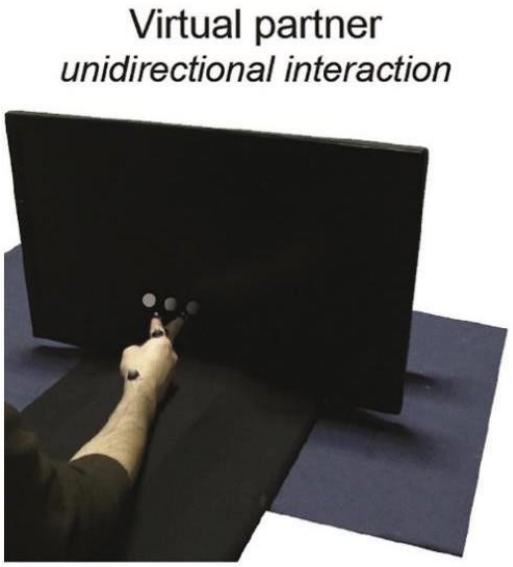

Figure 16. Experimental Setup and Procedure

Participants seated at a table with the ulnar side of the right forearm resting on a rigid support. They were asked to synchronize their movements to a visual dot that moved on a computer screen according to a pre-recorded human kinematics, either in-phase or anti-phase.

5.1.5 Kinematic data recording

Movements were recorded along three axes (mediolateral, X; anteroposterior, Y; and vertical, Z) using a ten cameras motion capture system (Vicon; Nexus; sampling rate: 300 Hz). Three retro-reflective markers were placed at the following anatomical locations on the right hand: on the distal phalanx of the index finger (marker diameter: 6.4 mm), on the metacarpophalangeal joint (marker diameter: 9.5 mm) and on the styloid process of the radius (marker diameter: 9.5 mm). A photodiode (1 x 1 cm) was placed in the bottom right corner of the monitor and was used for accurately aligning the participants' recorded kinematics with the displayed dot. A white square was drawn on the screen at the position of the photodiode (hidden from view) in synchrony with the start of the dot motion. The signal from the photodiode was acquired with the same system used to record the kinematic data (i.e., Vicon; sampling rate: 1800 Hz).

5.1.6 Data collection

Data were collected in separate trials with short pauses in-between trials. Two 2.5 min long trials were recorded for each participant and condition (In-phase/Anti-phase). The two trials per condition were always performed in succession. Instructions about task/condition were provided verbally before each trial sequence, and the order of tasks and conditions was randomized across participants.

5.1.7 Quantification and Statistical Analysis

Analyses were performed within the MATLAB computing environment using custom-made code and the FieldTrip toolbox for filtering the data. Analysed data corresponds to position data along the main movement axis for the marker attached on the fingertip. Velocity has been computed as the first derivative of position and normalized (trial-wise) on maximal speed.

5.1.7.1 Time-domain analysis

Detection of individual movements

To estimate onset/offset of each individual movement, we low pass filtered (3 Hz, two-pass

Butterworth, third order) the position data before computing the velocity. Movement onset was defined as the first data sample of a segment equal to 1/4 of the instructed movement duration (0.5 s) where the velocity was positive (or negative, depending on movement direction); movement offset was defined as the first sample after at least half the instructed movement duration (1 s; exact time could be slightly changed according to individual movement duration) from movement onset where the velocity passed through zero. This algorithm was applied iteratively by sliding along the entire velocity time series. Data segmentation was visually checked for each time series and any error was manually corrected (<5%).

Cross-correlation

The cross-correlation analysis was performed on velocity as obtained by taking the first derivative of position data that were low-pass filtered at 40 Hz to remove high-frequency noise. For each couple (moving dot and real participant) and condition, we first took velocity segments corresponding approximately to individual movements, i.e., time-locked to specific movement onsets of both moving dot and real participant and with length equal to mean movement duration (velocity segments belonging to movements with duration > or < than mean duration ± 2.5 SD were discarded from the analysis). Velocity sign was adjusted to be positive in all segments. To remove the movement-locked components, we subtracted from each segment the average velocity profile across all the retained segments (subject-wise). After these common preprocessing steps, we computed the cross-correlation (normalized so that the autocorrelations at zero lag were identically 1) by aligning the moving dot and human partner' velocity segments in two different ways: 1) movement-aligned, i.e., keeping the data aligned to each movement onset of both moving dot and participant as just described , and 2) time- aligned, i.e., using the movement onsets of the moving dot as reference temporal markers to re-align the real partner's data (Figures 17A and 17B). Therefore, only the second type of alignment (time-aligned) preserved the real time relationship between the moving dot and real partner' velocities.

Submovement-locked analysis

For the submovement-locked analysis (Figures 17C and 17D), position data were low-pass filtered (4 Hz, two-pass Butterworth, third order) before computing velocity. Preprocessing of velocity data (i.e., segmentation, change of velocity sign, subtraction of the across-segments average) was identical to that described for the cross-correlation analysis. For the moving dot, we identified the submovements as local peaks in the velocity, i.e., data points

with values larger than neighbouring values (in each velocity segment). We then segmented the same moving dot as well as the real partner velocities based on the identified submovements (from - 0.6 to 0.6 s), providing with 'submovement-triggered' averages (Figure 17C). Finally, the submovement-aligned data were also used to estimate the probability of producing a submovement given a submovement produced by the moving dot. Specifically, we counted the number of submovements (local velocity peaks) for each time point (from -0.6 to 0.6 s) in the real partner's velocity segments (aligned to the moving dot submovements) and then divided these numbers by the total amount of analysed velocity segments (Figure 17D). In a similar way as performed in the cross-correlation analysis, submovements probabilities were computed for both time-aligned and movement-aligned velocity data segments. We then averaged the computed probabilities within 36 equally spaced and non-overlapping bins between - 0.6 and +0.6 s.

5.1.7.2 Statistical analysis

Time- vs movement-locking of submovements

We tested whether real partner' submovement probability depended on the (actual) time from moving dot submovements – and was therefore significantly different from what could be obtained if the moving dot and real partner' submovements were locked to the individual movement onsets – by performing two-tailed paired samples t-tests on the probabilities computed for time- vs. movement-aligned data. The obtained p-values were then corrected for multiple comparisons across time by means of the Bonferroni method. We compared submovement probabilities before vs. after time zero by applying paired samples t-tests on the maximal probabilities computed for all real partners in the respective time intervals (i.e., from - 0.6 to 0 s and from 0 to +0.6 s).

5.1.8 Results

The timing of the participants' submovements is tightly related to that of the dot submovements. However, both the cross-correlation (Figures 17A and 17B) as well as the submovement-locked (Figures 17C and 17D) profiles are marked by a highly asymmetrical pattern that contrasts with the symmetrical one observed for the real interaction in Study 2 and 3. Specifically, for the In-phase condition, submovement probability is systematically higher at times following than preceding the virtual partner's submovements ($p < 0.0001$, Figure 17D); though with a clear reduction in the strength of submovements modulation, a

similar trend can also be observed for the Anti-phase condition (virtual partner: $p = 0.061$; paired samples *t*-tests on maximal probabilities before vs after time zero). The reported pattern exactly fulfills what is expected based on the bidirectional and unidirectional nature of the real and virtual interaction, respectively.

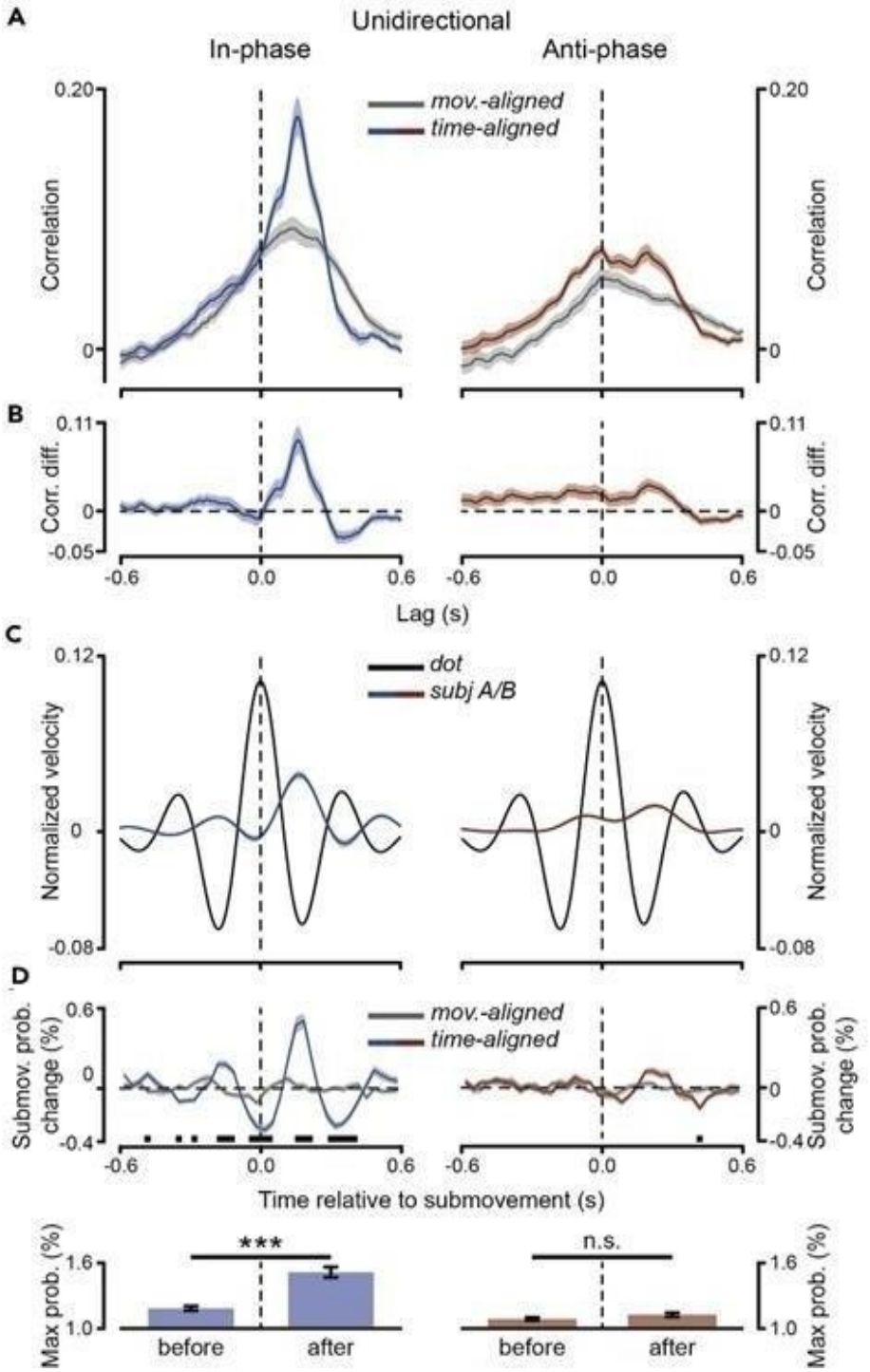

Figure 17. Unidirectional modulation of submovements.

A. Cross-correlation between the moving dot and real partner' (unfiltered) velocities during in-phase (left) and anti-phase (right) synchronization. The cross-correlation is computed between velocity data segments (~2 s) that are either movement-aligned, i.e., aligned to the respective movement onsets of moving dot and

participants or time-aligned, i.e., aligned to the moving dot movement onset, thus preserving their real time alignment (mean ± SEM).

B. Difference between the time- and movement-aligned cross-correlation profiles (mean ± SEM).

C. Velocity for both moving dot and real partner – locked to submovements generated by the moving dot (mean ± SEM).

D. Submovement probability (expressed as deviation from mean probability) for real partner as a function of the actual time (time-aligned) or of time relative to movement onset (movement-aligned) from submovements generated by moving dot. The black horizontal bars indicate the time points that survive two-tailed t-test statistics on movement- vs time-aligned data (Bonferroni-corrected for multiple comparisons across time). Maximal submovement probabilities (real partner time-aligned to moving dot) computed separately before and after time zero (i.e., before and after moving dot' submovements; bottom panels).

Chapter 6

6.1 Study 5. *Virtual motor coordination goal: Unimanual Task (Neurological patients)*

6.1.1 Abstract

Given the ease of transferability of the task to a clinical setting and the results obtained from our previous study (Study 4), we chose to evaluate the pattern of submovements emission in individuals with Parkinson's disease and cerebellar disorders. These disorders result in characteristic symptoms caused by dysfunction in the basal ganglia and cerebellum, respectively (see below for a brief description). We focused on these diagnostic categories because some authors suggest that the basal ganglia and cerebellum, due to their role in action selection, online correction and timing actions, might play a crucial role in intermittent motor control mechanisms (Loram et al., 2014). To improve the feasibility and cost-effectiveness of obtaining kinematic data related to submovements in a clinical setting, we chose to use a simple accelerometer instead of more complex and expensive technologies like motion capture systems. Our approach is supported by pilot data we collected on healthy subjects, as well as a study (Pereira et al., 2017) that examined submovements using acceleration profile. The data presented below is based on just three cases and is highly preliminary, serving as a proof of concept to demonstrate the feasibility of utilizing accelerometers to investigate submovements in a clinical setting. The ultimate goal of this approach is to identify new diagnostic markers and gain further knowledge about the neural substrates involved in movement intermittency.

6.1.2 Personal contribution

I implemented the experiment with my colleague Dr. Marco Emanuele, and I performed all the analyses using codes I wrote in Matlab under the supervision of Dr. Alice Tomassini and Prof. Alessandro D'Ausilio. The patients were recruited at Santa Lucia

Hospital in Rome with the collaboration of Prof. Giacomo Koch and Dr. Romina Esposito who collected the data.

6.1.3 Sample

The experiment involved three 67-years old participants (1 female). All participants reported being right-handed and had either normal or corrected-to-normal vision. Of the three participants, one was a healthy subject, while the other two had Parkinson's Disease (PD) and cerebellar disorder (CD) induced by a stroke, respectively. We cannot provide any further clinical information about the patients, as we are still in the data collection phase.

6.1.3.1 Parkinson's Disease

PD (Parkinson, 1817) is a widespread chronic neurological condition that typically affects older individuals, starting gradually and leading to significant disability. Historically, it was considered a disease of the extrapyramidal motor system and its primary motor symptoms include tremors at rest, slow and limited movement, stiffness, and postural instability. The hallmark of PD is the presence of intracellular inclusions of eosinophilic material known as Lewy bodies, found within dopamine-containing neurons in the substantia nigra. The progressive degeneration and decline of dopamine neurons in the nigrostriatal tract, particularly those destined for the putamen, leads to dopaminergic denervation in the basal ganglia and striatum, causing the distinctive motor symptoms: tremor, enhanced tone, bradykinesia (slowness of movement or progressive hesitation), and hypokinesia (abnormally diminished motor activity). However, the exact mechanisms underlying these symptoms are still not fully understood as well is the functional role of dopaminergic receptors, particularly D1.

6.1.3.2 Cerebellar disorders

Cerebellar disorders (CD) can have hereditary or sporadic origins and their symptoms depend on the extent and site of cerebellar damage. The cerebellum plays a crucial role in coordination, sensory integration, motor learning, and adaptation, therefore cerebellar dysfunction may result in symptoms such as unsteadiness and poor coordination. People

with CD may also exhibit characteristic gait variability due to a combination of balance impairments, difficulties coordinating limbs, and inconsistent coordination between posture and leg movements (Marsden, 2018). Based on anatomical divisions, cerebellar disorders can be divided into three classic syndromes: Damage to the lower vermis, also referred to as the vestibulocerebellum or archicerebellum, results in the flocculonodular syndrome. This condition can be caused by brain tumors, stroke, or bleeding from a blood vessel, leading to unsteadiness in posture, including swaying of the head and trunk while sitting, standing, or walking. Damage to the anterior lobe of the cerebellum results in the paleocerebellar syndrome, characterized by unsteady gait and difficulty maintaining balance while standing. Unlike patients with the vermis syndrome, individuals with the paleocerebellar syndrome use their eyes to stabilize themselves and tend to fall more often when their eyes are closed. They may also have dysarthria and dysmetric saccades, but generally have relatively preserved fine motor movements of the upper limbs. Finally, damage to the cerebellar hemispheres or their connecting pathways results in the neocerebellar syndrome, with poor coordination of the extremities, also known as limb ataxia. This can be due to causes such as strokes, occlusion of the superior cerebellar artery, brain tumors, or degenerative disorders, and may occur bilaterally or unilaterally. The severe disturbance of limb movements includes decreased muscle tone (hypotonia), poor timing of sequential movements (asynergia), and difficulties in coordinated changes in muscle activation (dysdiadochokinesia), with a severe tremor sometimes appearing during motor tasks (Goetz & Korchounov, 2014).

6.1.4 Procedure

Participants were seated at a table in front of a computer screen, with the ulnar side of their right forearm resting on a rigid support. They were asked to perform flexion-extension movements of their index finger about the metacarpophalangeal joint, while tracking a visual dot (size: 1.5 cm, position: 7 cm above the bottom screen edge) that moved horizontally on a computer screen in front of them (Figure 18). The dot velocity corresponded to the velocity of the index fingertip recorded on author A.T. while she was taking part in the solo performance of the primary task described in Study 2. Depending on the condition, participants were asked to track the dot kinematics either in-phase or anti-phase.

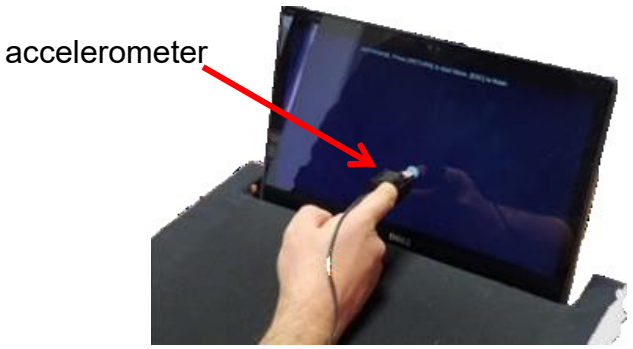

Figure 18. Experimental Setup and Procedure. Participants seated at a table with the ulnar side of the right forearm resting on a rigid support. They were asked to synchronize their movements to a visual dot that moved horizontally on a computer screen according to a pre-recorded human kinematics, either in-phase or anti-phase.

6.1.5 Kinematic data recording

Movements were recorded along three axes (anteroposterior, X; vertical, Y and mediolateral Z) using an accelerometer (InvenSense MPU-6050; sampling rate: 60 Hz) posited on the palmar side of the distal phalanx of participants' right index finger.

6.1.6 Data collection

Data were collected in separate trials with short pauses in-between trials. Three 1.5 min long trials were recorded for each participant and condition (in-phase/anti-phase). The three trials per condition were always performed in succession. Instructions about task/condition were provided verbally before each trial sequence, and the order of conditions was randomized across participants.

6.1.7 Time Domain Analysis

Analyses were performed within the MATLAB computing environment using custom-made code and the FieldTrip toolbox for filtering the data. Analysed data corresponds to accelerometer data along the main movement axis (Z).

Detection of individual movements

Dot

To estimate onset/offset of each individual movement of the pre-recorded human kinematic, we low pass filtered (3 Hz, two-pass Butterworth, third order) the position data before computing the velocity. Movement onset was defined as the first data sample of a segment equal to 1/4 of the instructed movement duration (0.5 s, see) where the velocity was positive (or negative, depending on movement direction); movement offset was defined as the first sample after at least half the instructed movement duration (1 s) from movement onset where the velocity passed through zero. This algorithm was applied iteratively by sliding along the entire velocity time series.

Participants

The onset of each flexion/extension movement was determined using low-pass filtered (0.6 Hz, two-pass Butterworth, third order) acceleration data. Movement onsets were defined as peaks in acceleration data that corresponded to a change in movement direction, i.e., from flexion to extension or vice versa. Peaks were detected on acceleration data where the sign was adjusted to be positive in all recorded trials. All errors in data segmentation were manually corrected: Segments in which participants lost the coordination mode with the movement of the dot were removed from the analysis.

Segmentation

The previously identified timestamps of movement onset were used to segment the acceleration data for both the moving dot and participants. The acceleration data for the moving dot was calculated as the second derivative of the position data. All analyses (described below) were performed on band-pass filtered acceleration data (two-pass Butterworth filter, third order) in the submovement range of 1.5-4.5 Hz and preprocessed as follows:

1. The sign of the acceleration segments was adjusted to ensure that all acceleration segments were positive (first step: change of acceleration sign).
2. The acceleration was normalized to a range of values spanning from -1 to +1 (second step: acceleration normalization).

3. The average acceleration profile was subtracted from each acceleration segment to remove movement-related components (third step: average acceleration profile subtraction).

Submovement-locked analysis (qualitative analysis)

For the submovement-locked analysis (Figure 19), we identified submovements as local peaks in the acceleration segments of the moving dot. We then segmented the acceleration data for both the moving dot and participants based on the identified submovements, within a time window of ±0.6 seconds. In this way, we defined acceleration segments (for both the moving dot and participants) centred around the submovements detected in the acceleration profile of the moving dot. Importantly, the acceleration segments of participants were preliminarily time-aligned with the movement onsets of the moving dot to restore the actual temporal relationship between the movements of the dot and the participants as they occurred during the experiment.

6.1.8 Results

The qualitative analysis of the graphs resulting from the submovement-locked analysis shows a pattern of results for the healthy control group that is comparable to those found in the previous study (Study 4) on healthy young subjects. In the In-phase Condition, the submovements emitted by the participant systematically follows that of the moving dot to which they are time-locked, while in the Anti-phase Condition, this modulation seems to be almost completely absent. Indeed, there is no clear temporal relationship between the participant's submovements and the corresponding submovements emitted by the moving dot. Surprisingly, both patients show a pattern of results opposing to those observed in healthy control. In the In-phase Condition, it is not possible to appreciate any temporal relationship between the submovements emitted by the moving dot and those correspondingly emitted by the patients, as evidenced by the almost flat profile of the patients' submovements. In contrast, in the Anti-phase Condition, although less markedly than observed in the In-phase Condition of healthy control, a slight modulation in the emission of submovements by the patients is detectable. In this case, it appears that the submovements emitted by the patients systematically follow those emitted by the moving dot to which they are time-locked. These results, although extremely preliminary, could lead us to conclude that patients, whether suffering from cerebellar disorders or Parkinson's disease, show somewhat altered patterns of visual-based movement correction

compared to healthy control.

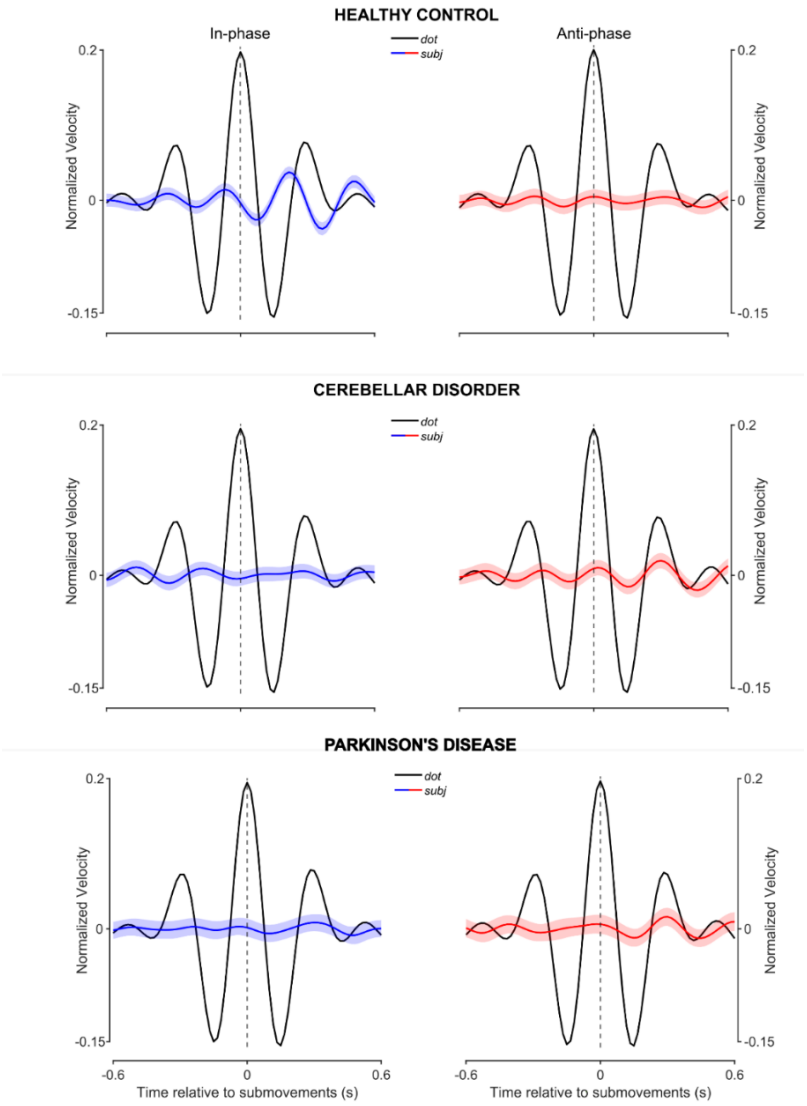

Figure 19 Temporal dynamics of submovements modulation

Acceleration profile of moving dot and single subjects time-locked to submovements emitted by the dot that moved according to a pre-recorded human kinematic for both In-phase and Anti-phase Conditions.

Discussion

In this thesis, I reported investigations about the temporal patterns of submovements emission in various bimanual and unimanual coordination tasks performed by individual subjects or pairs of interacting subjects. Through the identification of different temporal emission patterns of submovements, we can conclude that the mechanisms controlling submovement production are highly flexible and tunable, depending on the objectives, mode, and intrapersonal or interpersonal context in which coordination takes place. Furthermore, the type of temporal relationship between submovements seems to vary depending on the availability of visual and/or proprioceptive feedback and their usability for updating and correcting the motor program in real-time.

7.1 Patterns of submovements emission during bimanual and interpersonal motor coordination task

In Study 1, we analyzed the temporal relationship between submovements emitted by the two hands of a single participant who was engaged in a bimanual coordination task. Our findings revealed that, regardless of the coordination mode (in-phase or anti-phase), the submovements emitted by the two hands showed a complex relationship of anticipation and simultaneity when the subject observed their own movements. However, when the subject closed their eyes, the submovements produced by the two hands were emitted almost simultaneously in both coordination modes. This suggests that isochrony in submovement emission might depend on a single controller that regulates movement encoding (as described by Merrick et al., 2022). This controller produces motor micro-adjustments at regular intervals to accommodate positional errors in the endpoints of index fingers of both hands, which are signaled by proprioceptive information.

Consistently, previous studies have shown that proprioceptive information, which is related to body position and derived from sense organs in muscles and joints, can be used for online correction of movement errors during reaching tasks (Gosselin-Kessiby et al., 2009). However, the reappearance of visual feedback may have disrupted the isochrony relationship, causing submovement output to shift from a clock-driven to an event-driven or adaptive intermittent mode (Sakaguchi et al., 2015). Visual feedback could have made the temporal relationship between the submovements of the two hands more sparse and complex

because positional errors between the endpoints of the two hands, which are signaled by visual feedback, could occur more irregularly. As a result, motor micro-adjustments are produced whenever a certain threshold of error is exceeded, but this threshold will never be constant. Overall, the more articulated pattern of temporal relationship between the submovements of the two hands when visual and proprioceptive feedback are co-present could reflect a complex multisensory integration process, for which some models have been proposed. (Kasuga et al., 2022).

Surprisingly, in both the unimanual task (Study 2) and the bimanual task (Study 3), we found that the submovements emitted by the hands of two interacting participants alternate over time and are time-locked to each other (Tomassini et al., 2022). This suggest that submovements are coupled between interacting partners, reflecting a process of active co-regulation and mutual adaptation. During interactions, visuomotor control cannot be limited to a single individual but it must include feedback related to both one's own and the partner's actions. As a result, the visual error signal becomes a co-product of both the self's and the other's movements. However, the relationship between submovements is closely related to the coordination mode at the movement level: it is apparent during in-phase coordination but almost absent during anti-phase coordination. This distinction persists regardless of hand posture or dominance and is likely due to the visuospatial constraints inherent in the two modes of coordination. Anti-phase movement involves a larger spatial distance between endpoints than in-phase movement, which can result in more imprecise, less reliable, and potentially delayed computation of visual errors. Previous research has indicated that visual errors play a significant role in shaping movement intermittency. Increasing the spatial separation between the target and hand cursor has been found to decrease intermittency and tracking accuracy. This is probably due to the coarser visual evaluation of positional errors, resulting in less precise feedback-based motor adjustments (Reed et al., 2003). Estimating the positional visual error of the two fingertip endpoints during anti-phase coordination is inherently difficult and may result in a broader "error dead zone" - referring to the range of inputs that the motor system is unresponsive to, preventing any updates to motor commands (Wolpert et al., 1993).

Moreover, shortening movement duration and increasing speed beyond a certain limit impairs online motor corrections, negatively affecting interpersonal submovement coordination. These constraints (movement duration and coordination mode) are consistent with functional constraints arising from feedback-based motor control mechanism. It is noteworthy that when we examine the relationship between submovements emitted by single participants' both hands while coordinating with their partner, we found the same

pattern of results as when participants coordinate their fingers with their eyes closed (Study 1). In this situation, it is possible that submovement emission is produced by a single controller that seeks to accommodate the submovements of the interacting partner. Similarly to the eyes-closed condition, the participant is "blind" to the spatial relationship between their own fingers because the focus of observation and spatial error to be corrected is connected to the partner's finger position with whom (s)he is trying to coordinate. The isochrony observed between submovements may depend on intermittent resampling of the visual scene, which provides the necessary feedback to update the motor plan and promote in-phase and anti-phase coordination with the partner at regular intervals. A growing body of evidence indeed suggests that sampling of sensory data may operate in an intermittent, rhythmic manner (VanRullen, 2016) and can be strictly coupled to motor behavior (Tomassini & D'Ausilio, 2018; Nakayama & Motoyoshi, 2019; Benedetto et al., 2020). Specifically, fluctuations in visual perception are synchronized not only with eye movements, but also with oscillations in neural activity related to the planning and monitoring of upper limb movements (Benedetto et al., 2021; Tomassini et al., 2020).

Overall, as indicated in Table 1, the coordination pattern of submovements is differentially influenced by the availability and usability of visual and proprioceptive feedback, depending on the level of analysis (between or within subjects) and coordination mode (in-phase or anti-phase). Specifically, visual feedback is available and usable for updating the motor program in all tasks, except for the eyes closed condition in Study 1 and when analysing the relationship between submovements of both hands of a single participant in Study 3. In this latter case, visual feedback is available but not effectively used for updating the motor program because the focus of observation is on the spatial relationship of one's own fingers with those of the interacting partner. On the other hand, proprioceptive feedback is always available, but it is only effectively used to update the motor program in Study 1. In Studies 2-3, updating the motor program is a joint product of the relationship with the other, which is mediated primarily by vision.

Coordination Goal	Interpersonal				Intrapersonal			
Level of Analysis	Between Subjects		Within Subjects		Within Subjects			
Task	Unimanual & Bimanual		Bimanual		Bimanual			
Visual Feedback (Availability and Usability)	Yes		No		Yes		No	
Proprioceptive Feedback (Usability)	No		No		Yes		Yes	
Coordination mode	In-phase	Anti-phase	In-phase	Anti-phase	In-phase	Anti-phase	In-phase	Anti-phase
Pattern of submovements coordination	Alternation	No Clear Relation	Quasi-simultaneity		Mixture of alternation and simultaneity		Quasi-simultaneity	

Table 1 Summary of the results for Study 1-3.

Finally, it is important to note that submovements are present not only during dyadic coordination, but also during solo performances that only require temporal accuracy, thus reducing the need for online visual-based motor corrections. This is in accordance with studies showing that submovements are not nullified or reduced even whenvisual feedback is completely absent (Doeringer & Hogan, 1998; Vallbo & Wessberg, 1993). Therefore, this supports an alternative explanation that considers submovements as an intrinsic property or dynamic primitive of movement organization (Hogan & Sternad, 2012).

7.2 Pattern of submovements emission during virtual interaction

When interacting with an unresponsive virtual partner, the temporal symmetry is disrupted, and participants' submovements more often follow the dot's submovements rather than precede them, especially during in-phase coordination mode. This finding suggests that the discontinuities in the dot motion “drives” participants’ submovements, offering a depiction of the “normative” pattern of submovements emission while tracking the motion of a virtual partner. Importantly, the same pattern of results, which was replicated in a healthy elderly participant was not evident in two subjects affected by Parkinson's disease (PD) and cerebellar disorder (CD). This is not surprising given the complementary roles that the basal ganglia and cerebellum, which are respectively affected in PD and CD, play in regulating ongoing actions when precise updating is required (Tunik et al., 2009). However, if these results will be replicated in a larger sample of healthy elderly subjects and those affected by

PD and CD, they could provide converging evidence regarding the neurophysiological role of the basal ganglia and cerebellum in submovement production. Moreover, these findings could have significant clinical relevance and be used as objective diagnostic and prognostic markers to assess disease progression in a simple and cost-effective manner.

7.3 Conclusion

In conclusion the present findings suggest that the mechanism responsible for the organization of movement into submovements is at least partly shared across different effectors, such as the two hands. Submovements control can thus provide key insights onto the low-level motor control mechanisms that are differentially exploited to achieve bimanual and interpersonal coordination. The distinct pattern of submovements emission indeed posit for an highly tuneable mechanism adapting to different coordinative challenges. More generally, intermittency, underlying submovements emission could represent a fundamental mechanism of sensorimotor functions underlying voluntary behaviour and the availability (and usability) of visual and proprioceptive feedback is of crucial importance for applying task-relevant (micro)motor corrections. Thus saying submovements-level control may serve as a novel objective marker of individual and social motor coordination capabilities that may be selectively impaired in psychiatric and neurological disorders. Further studies, however, are needed to provide more insight into this question, as well as to elucidate how leader-follower dynamics in interpersonal coordination or hand dominance in bimanual coordination could impact the observed temporal relationship between submovements.

Bibliography

Benedetto, A., Binda, P., Costagli, M., Tosetti, M., & Morrone, M. C. (2021). Predictive visuo-motor communication through neural oscillations. *Current Biology*, *31*(15), 3401-3408.

Benedetto, A., Morrone, M. C., & Tomassini, A. (2020). The common rhythm of action and perception. *Journal of cognitive neuroscience*, *32*(2), 187-200.

Bernieri, F. J., & Rosenthal, R. (1991). Interpersonal coordination: Behavior matching and interactional synchrony. In *Fundamentals of nonverbal behaviour* (pp. 401–432). Cambridge University Press. Bressler, S. L., & Kelso, J. A. S. (2001). Cortical coordination dynamics and cognition. *Trends in Cognitive Sciences*, *5*(1), 26–36.

Cattaert, D., Semjen, A., & Summers, J. J. (1999). Simulating a neural cross-talk model for between-hand interference during bimanual circle drawing. *Biological Cybernetics*, *81*(4), 343–358.

Colomer, C., Dhamala, M., Ganesh, G., & Lagarde, J. (2022). Interacting humans use forces in specific frequencies to exchange information by touch. *Scientific Reports*, *12*(1), Art. 1.

Condon, W. S., & Ogston, W. D. (1967). A segmentation of behaviour. *Journal of Psychiatric Research*,*5*(3), 221–235.

Craik, K. J. (1947). Theory of the human operator in control systems 1: I. The operator as an engineering system. *British Journal of Psychology. General Section*, *38*(2), 56-61.

Czeszumski, A., Eustergerling, S., Lang, A., Menrath, D., Gerstenberger, M.,

Schuberth, S., Schreiber, F., Rendon, Z. Z., & König, P. (2020). Hyperscanning: a valid method to study neural inter-brain underpinnings of social interaction. *Frontiers in Human Neuroscience*, *14*, 39.

Doeringer, J. A., & Hogan, N. (1998). Intermittency in Preplanned Elbow Movements Persists in the Absence of Visual Feedback. *Journal of Neurophysiology*, *80*(4), 1787–1799.

Dounskaia, N., Wisleder, D., & Johnson, T. (2005). Influence of biomechanical factors on substructure of pointing movements. *Experimental Brain Research*, *164*(4), 505–516.

Dumas, G., Nadel, J., Soussignan, R., Martinerie, J., & Garnero, L. (2010). Inter-Brain Synchronization during Social Interaction. *PLOS ONE*, *5*(8), e12166.

Era, V., Boukarras, S., & Candidi, M. (2019). Neural correlates of action monitoring and mutual adaptation during interpersonal motor coordination: Comment on «The body talks: Sensorimotor communication and its brain and kinematic signatures» by G. Pezzulo et al. *Physics of Life Reviews*,*28*, 43–45.

Franz, E. A., Eliassen, J. C., Ivry, R. B., & Gazzaniga, M. S. (1996). Dissociation of Spatial and Temporal Coupling in the Bimanual Movements of Callosotomy Patients. *Psychological Science*, *7*(5), 306–310.

Franz, E. A., Waldie, K. E., & Smith, M. J. (2000). The Effect of Callosotomy on Novel Versus Familiar Bimanual Actions: A Neural Dissociation Between Controlled and Automatic Processes? *Psychological Science*, *11*(1), 82–85.

Gawthrop, P., Gollee, H., Lakie, M., & Loram, I. D. (2022). Intermittent Control of Movement and Balance. In D. Jaeger & R. Jung (A c. Di), *Encyclopedia of Computational Neuroscience* (pp. 1689–1694). Springer.

Gawthrop, P., Loram, I., Lakie, M., & Gollee, H. (2011). Intermittent control: A computational theory of human control. *Biological Cybernetics*, *104*(1), 31–

51.

Goetz, C. G., & Korchounov, A. (2014). Cerebellar Disorders. In M. J. Aminoff & R. B. Daroff (A c. Di),*Encyclopedia of the Neurological Sciences (Second Edition)* (pp. 641–642). Academic Press.

Gooijers, J., & Swinnen, S. P. (2014). Interactions between brain structure and behaviour: The corpus callosum and bimanual coordination. *Neuroscience and Biobehavioural Reviews*,*43*, 1–19.

Gross, J., Timmermann, L., Kujala, J., Dirks, M., Schmitz, F., Salmelin, R., & Schnitzler, A. (2002). The neural basis of intermittent motor control in humans. *Proceedings of the National Academy of Sciences of the United States of America*, *99*(4), 2299.

Hall, T. M., de Carvalho, F., & Jackson, A. (2014). A Common Structure Underlies Low-Frequency Cortical Dynamics in Movement, Sleep, and Sedation. *Neuron*, *83*(5), 1185–1199.

Harris, C. M., & Wolpert, D. M. (1998). Signal-dependent noise determines motor planning. *Nature*,*394*(6695), Art. 6695.

Hogan, N., & Sternad, D. (2012). Dynamic primitives of motor behaviour. *Biological Cybernetics*,*106*(11), 727–739.

Houk, J. C., Bastianen, C., Fansler, D., Fishbach, A., Fraser, D., Reber, P. J., Roy, S. A., & Simo, L. S. (2007). Action selection and refinement in subcortical loops through basal ganglia and cerebellum. *Philosophical Transactions of the Royal Society B: Biological Sciences*, *362*(1485), 1573–1583.

Jerbi, K., Lachaux, J.-P., N′Diaye, K., Pantazis, D., Leahy, R. M., Garnero, L., & Baillet, S. (2007). Coherent neural representation of hand speed in humans revealed by MEG imaging. *Proceedings of the National Academy of Sciences*, *104*(18), 7676–7681.

Kawato, M. (1999). Internal models for motor control and trajectory planning. *Current Opinion inNeurobiology*, *9*(6), 718–727.

Keller, P. E., Novembre, G., & Hove, M. J. (2014). Rhythm in joint action: Psychological and neurophysiological mechanisms for real-time interpersonal coordination. *Philosophical Transactions of the Royal Society B: Biological Sciences*, *369*(1658), 20130394.

Kelso, J. S. (1995). *Dynamic patterns: The self-organization of brain and behavior*. MIT press.

Kokal, I., Engel, A., Kirschner, S., & Keysers, C. (2011). Synchronized Drumming Enhances Activity in the Caudate and Facilitates Prosocial Commitment—If the Rhythm Comes Easily. *PLOS ONE*, *6*(11), e27272.

Launay, J., Dean, R. T., & Bailes, F. (2013). Synchronization Can Influence Trust Following Virtual Interaction. *Experimental Psychology*, *60*(1), 53–63.

Lindenberger, U., Li, S.-C., Gruber, W., & Müller, V. (2009). Brains swinging in concert: Cortical phase synchronization while playing guitar. *BMC Neuroscience*, *10*(1), 22.

Loram, I. D., Gollee, H., Lakie, M., & Gawthrop, P. J. (2011). Human control of an inverted pendulum: Is continuous control necessary? Is intermittent control effective? Is intermittent control physiological? *The Journal of Physiology*, *589*(2), 307–324.

Loram, I. D., van de Kamp, C., Lakie, M., Gollee, H., & Gawthrop, P. J. (2014). Does the Motor System Need Intermittent Control? *Exercise and Sport Sciences Reviews*, *42*(3), 117.

Louwerse, M. M., Dale, R., Bard, E. G., & Jeuniaux, P. (2012). Behaviour Matching in Multimodal Communication Is Synchronized. *Cognitive Science*, *36*(8), 1404–1426.

Marsden, J. F. (2018). Chapter 17—Cerebellar ataxia. In B. L. Day & S. R. Lord (A c. Di), *Handbook of Clinical Neurology* (Vol. 159, pp. 261–281). Elsevier.

Miall, R. C. (1996). Task-Dependent Changes in Visual Feedback Control: A Frequency Analysis of Human Manual Tracking. *Journal of Motor Behaviour*, *28*(2), 125–135.

Miles, L. K., Nind, L. K., Henderson, Z., & Macrae, C. N. (2010). Moving memories: Behavioural synchronyand memory for self and others. *Journal of Experimental Social Psychology*, *46*(2), 457–460.

Müller, V., Ohström, K.-R. P., & Lindenberger, U. (2021). Interactive brains, social minds: Neural and physiological mechanisms of interpersonal action coordination. *Neuroscience & Biobehavioural Reviews*, *128*, 661–677.

Nakayama, R., & Motoyoshi, I. (2019). Attention Periodically Binds Visual Features As Single Events Depending on Neural Oscillations Phase-Locked to Action. *Journal of Neuroscience*, *39*(21), 4153–4161.

Néda, Z., Ravasz, E., Brechet, Y., Vicsek, T., & Barabási, A. L. (2000). The sound of many hands clapping. *Nature*, *403*(6772), 849-850.

Novembre, G., Sammler, D., & Keller, P. E. (2016). Neural alpha oscillations index the balance between self- other integration and segregation in real-time joint action. *Neuropsychologia*, *89*, 414–425.

Pereira, M., Sobolewski, A., & Millán, J. del R. (2017). Action Monitoring Cortical Activity Coupled to Submovements. *Eneuro*, *4*(5), ENEURO.0241-17.2017.

Pezzulo, G., Donnarumma, F., Dindo, H., D'Ausilio, A., Konvalinka, I., & Castelfranchi, C. (2019). The body talks: Sensorimotor communication and its brain and kinematic signatures. *Physics of LifeReviews*, *28*, 1–21.

Rabinowitch, T.-C., & Meltzoff, A. N. (2017). Joint Rhythmic Movement Increases 4-Year-Old Children's Prosocial Sharing and Fairness Toward Peers. *Frontiers in Psychology*, *8*.

Richardson, M. J., Marsh, K. L., & Schmidt, R. C. (2005). Effects of Visual and Verbal Interaction on Unintentional Interpersonal Coordination. *Journal of Experimental Psychology: Human Perceptionand Performance*, *31*, 62–79.

Sakaguchi, Y., Tanaka, M., & Inoue, Y. (2015). Adaptive intermittent control: A computational model explaining motor intermittency observed in human behaviour. *Neural Networks*, *67*, 92–109.

Sänger, J., Lindenberger, U., & Müller, V. (2011). Interactive brains, social minds. *Communicative &Integrative Biology*, *4*(6), 655–663.

Schmidt, R. C., Carello, C., & Turvey, M. T. (1990). Phase transitions and critical fluctuations in the visual coordination of rhythmic movements between people. *Journal of Experimental Psychology: Human Perception and Performance*, *16*, 227–247.

Sebanz, N., Bekkering, H., & Knoblich, G. (2006). Joint action: Bodies and minds moving together. *Trendsin Cognitive Sciences*, *10*(2), 70–76.

Sebanz, N., & Knoblich, G. (2009). Prediction in Joint Action: What, When, and Where. *Topics in CognitiveScience*, *1*(2), 353–367.

Semjen, A., & Ivry, R. B. (2001). The coupled oscillator model of between-hand coordination in alternate- hand tapping: A reappraisal. *Journal of Experimental Psychology: Human Perception and Performance*, *27*, 251–265.

Sherwood, D. E. (1994). Hand Preference, Practice Order, and Spatial Assimilations in Rapid BimanualMovement. *Journal of Motor Behaviour*, *26*(2), 123–134.

Shockley, K., Baker, A. A., Richardson, M. J., & Fowler, C. A. (2007).

Articulatory constraints on interpersonal postural coordination. *Journal of Experimental Psychology: Human Perception and Performance*, *33*, 201–208.

Summers, J. J., Rosenbaum, D. A., Burns, B. D., & Ford, S. K. (1993). Production of polyrhythms. *Journal of Experimental Psychology: Human Perception and Performance*, *19*, 416–428.

Susilaradeya, D., Xu, W., Hall, T. M., Galán, F., Alter, K., & Jackson, A. (2019). Extrinsic and intrinsic dynamics in movement intermittency. *ELife*, *8*, e40145.

Swinnen, S. P., & Gooijers, J. (2015). Bimanual coordination. In A. W. Toga (A c. Di), *Brain mapping: an encyclopedic reference*, *2*, 475-482. Academic Press.

Swinnen, S. P., & Wenderoth, N. (2004). Two hands, one brain: cognitive neuroscience of bimanual skill. *Trends in cognitive sciences*, *8*(1), 18-25.

Tarr, B., Launay, J., & Dunbar, R. I. M. (2016). Silent disco: Dancing in synchrony leads to elevated pain thresholds and social closeness. *Evolution and Human Behaviour*, *37*(5), 343–349.

Tomassini, A., & D'Ausilio, A. (2018). Passive sensorimotor stimulation triggers long lasting alpha-band fluctuations in visual perception. *Journal of Neurophysiology*, *119*(2), 380–388.

Tomassini, A., Laroche, J., Emanuele, M., Nazzaro, G., Petrone, N., Fadiga, L., & D'Ausilio, A. (2022). Interpersonal synchronization of movement intermittency. *Iscience*, *25*(4), 104096.

Tomassini, A., Maris, E., Hilt, P., Fadiga, L., & D'Ausilio, A. (2020). Visual detection is locked to the internal dynamics of cortico-motor control. *PLOS Biology*, *18*(10), e3000898.

Torricelli, F., Tomassini, A., Pezzulo, G., Pozzo, T., Fadiga, L., & D'Ausilio, A. (2022). Motor invariants in action execution and perception. *Physics of Life*

Reviews, *44*, 13–47.

Valdesolo, P., Ouyang, J., & DeSteno, D. (2010). The rhythm of joint action: Synchrony promotes cooperative ability. *Journal of Experimental Social Psychology*, *46*(4), 693–695.

Vallbo, A. B., & Wessberg, J. (1993). Organization of motor output in slow finger movements in man. *TheJournal of Physiology*, *469*(1), 673–691.

Van De Kamp, C., Gawthrop, P., Gollee, H., Lakie, M., & Loram, I. (2013). Interfacing sensory input with motor output: Does the control architecture converge to a serial process along a single channel? *Frontiers in Computational Neuroscience*, *7*.

VanRullen, R. (2016). Perceptual Cycles. *Trends in Cognitive Sciences*, *20*(10), 723–735.

Vesper, C., Abramova, E., Bütepage, J., Ciardo, F., Crossey, B., Effenberg, A., Hristova, D., Karlinsky, A., McEllin, L., Nijssen, S. R. R., Schmitz, L., & Wahn, B. (2017). Joint Action: Mental Representations, Shared Information and General Mechanisms for Coordinating with Others. *Frontiers in Psychology*, *7*.

Vince, M. A. (1948). The intermittency of control movements and the psychological refractory period. *British Journal of Psychology*, *38*(3), 149-157.

Wolpert, D., Miall, R. C., Winter, J., & Stein, J. (1993). Evidence for an Error Deadzone in Compensatory Tracking. *Journal of motor behaviour*, *24*, 299–308.

Wolpert, D. M. & Bastian, A. J. (2021). Principles of Sensorimotor Control. In Kandel, E. R., Koester, J. D., Mack, S. H., & Siegelbaum, S. A. *Principles of Neural Science, 6e* (Vol. 1–Book, Section). McGraw Hill.

Woodworth, R. S. (1899). Accuracy of voluntary movement. *The Psychological Review: MonographSupplements*, *3*(3), 1–114.